Journal of Anatomy

J. Anat. (2018) **232**, pp604–640 doi: 10.1111/joa.12775

Developmental patterns and variation among early theropods

C. T. Griffin

Department of Geosciences, Virginia Tech, Blacksburg, VA, USA

Abstract

Understanding ontogenetic patterns is important in vertebrate paleontology because the assessed skeletal maturity of an individual often has implications for paleobiogeography, species synonymy, paleobiology, and body size evolution of major clades. Further, for many groups the only means of confidently determining ontogenetic status of an organism is through the destructive process of histological sampling. Although the ontogenetic patterns of Late Jurassic and Cretaceous dinosaurs are better understood, knowledge of the ontogeny of the earliest dinosaurs is relatively poor because most species-level growth series known from these groups are small (usually, maximum of $n \sim 5$) and incomplete. To investigate the morphological changes that occur during ontogeny in early dinosaurs, I used ontogenetic sequence analysis (OSA) to reconstruct developmental sequences of morphological changes in the postcranial ontogeny of the early theropods *Coelophysis bauri* and *Megapnosaurus rhodesiensis*, both of which are known from large sample sizes ($n = 174$ and 182, respectively). I found a large amount of sequence polymorphism (i.e. intraspecific variation in developmental patterns) in both taxa, and especially in *C. bauri*, which possesses this variation in every element analyzed. *Megapnosaurus rhodesiensis* is similar, but it possesses no variation in the sequence of development of ontogenetic characters in the tibia and tarsus. Despite the large amount of variation in development, many characters occur consistently earlier or later in ontogeny and could therefore be important morphological features for assessing the relative maturity of other early theropods. Additionally, there is a phylogenetic signal to the order in which homologous characters appear in ontogeny, with homologous characters appearing earlier or later in developmental sequences of early theropods and the close relatives of dinosaurs, silesaurids. Many of these morphological features are important characters for the reconstruction of archosaurian phylogeny (e.g. trochanteric shelf). Because these features vary in presence or appearance with ontogeny, these characters should be used with caution when undertaking phylogenetic analyses in these groups, since a specimen may possess certain character states owing to ontogenetic stage, not evolutionary relationships.

Key words: bone scar; dinosaur; intraspecific variation; Jurassic; morphological maturity; ontogeny; theropod; Triassic.

Introduction

Understanding morphological changes undergone by an organism during ontogeny is a well-recognized problem in vertebrate paleontology, especially in extinct reptiles, which often lack easily discernible anatomical indicators of age (Johnson, 1977; Galton, 1982; Raath, 1990; Bennett, 1993, 1996; Brochu, 1996; Carr, 1999; Irmis, 2007; Delfino & Sánchez-Villagra, 2010; Piechowski et al. 2014; Griffin & Nesbitt, 2016a). Because the biology of extinct organisms may differ from their closest extant relatives in unexpected or unique ways, using extant analogues has an important but limited value for understanding how extinct organisms grew, and how those developmental patterns have evolved through time (e.g. Irmis, 2007). However, ontogenetic studies using extinct taxa, especially in older or rarer groups (e.g. early bird-line archosaurs), are often hampered by a dearth of ontogenetic series of species-level specimens, and those series that are available often have a limited sample size (often, a maximum of $n \sim 5$ for early bird-line archosaurs).

Studies of Late Jurassic and Cretaceous dinosaurian ontogenies are relatively common and have been utilized with great success to understand such questions as species synonymy (e.g. Madsen, 1976; Carr, 1999; Horner & Goodwin, 2009; Scanella & Horner, 2010; Novas et al. 2015) which in

Correspondence
Christopher T. Griffin, Department of Geosciences, Virginia Tech, Blacksburg, VA, USA.
E: ctgriff@vt.edu

Accepted for publication *7 December 2017*
Article published online *23 January 2018*

turn influences paleodiversity estimates and paleobiogeography, the evolution of growth rates and metabolism (Horner et al. 1999, 2000, 2001; Padian et al. 2001; Erickson et al. 2004; Horner & Padian, 2004), and mass-extinction structure and recovery (Codron et al. 2012). However, because of a comparative rarity of ontogenetic series, our understanding of the ontogenies of early dinosaurs is lacking, and our knowledge becomes increasingly poor in those clades closest to the origin of dinosaurs in the Late Triassic (Langer, 2004; Langer & Benton, 2006). The comparatively uncommon ontogenetic studies of Triassic and Early Jurassic dinosaurs have usually focused on osteohistology (Ricqlés, 1968; Chinsamy, 1990, 1993; Padian et al. 2004; Sander et al. 2004; Sander & Klein, 2005; Klein & Sander, 2007; Knoll et al. 2010) or allometry (Gay, 2005; Rinehart et al. 2009), with some studies undertaking a discussion of morphological or ontogenetic variation (Colbert, 1989, 1990; Raath, 1990; Genin, 1992; Benton et al. 2000; Tykoski, 2005; Griffin & Nesbitt, 2016b; Barta et al. 2018).

In this study, I describe postcranial variation in the early neotheropod dinosaurs *Coelophysis bauri* and *Megapnosaurus rhodesiensis* in detail, and place this variation in the context of the evolution of ontogenetic change in early theropods. *Coelophysis bauri* and *M. rhodesiensis* provide excellent study taxa to study morphological changes in ontogeny in early theropods and other dinosaurs because: (i) they have been reported to possess a high amount of variation in the presence of bone scars and co-ossifications (= bone 'fusions'; Raath, 1977, 1990; Colbert, 1989, 1990; Genin, 1992; Griffin & Nesbitt, 2016b; Barta et al. 2018), similar to non-dinosaurian dinosauriforms (Griffin & Nesbitt, 2016a,b); (ii) they are both early-diverging neotheropods, and therefore in a close phylogenetic position to the common dinosaurian ancestor, possessing many character states in common with this ancestor (Nesbitt et al. 2009b; Nesbitt, 2011; Sues et al. 2011); (iii) both *C. bauri* and *M. rhodesiensis* are temporally close (Late Triassic, Colbert, 1989; and Early Jurassic, Raath, 1977; respectively) to the origin of dinosaurs in the Late Triassic (Langer & Benton, 2006; Brusatte et al. 2010; but see Nesbitt et al. 2013 for a potential Middle Triassic origin); and (iv) they are both known from large ontogenetic series of varying sizes and states of morphological maturity, based on the state of ontogenetically variable characters (*sensu* Griffin & Nesbitt, 2016b).

Institutional abbreviations: AMNH FARB, American Museum of Natural History, New York, NY, USA; BMR, Burpee Museum of Natural History, Rockford, IL, USA; CM, Carnegie Museum of Natural History, Pittsburgh, PA, USA; CMNH, Cleveland Museum of Natural History, Cleveland, OH, USA; FMNH, Field Museum of Natural History, Chicago, IL, USA; GR, Ghost Ranch Ruth Hall Museum of Paleontology, Abiquiu, NM, USA; HMN, Museum für Naturkunde, Humboldt Universität, Berlin, Germany; MCZ, Museum of Comparative Zoology, Harvard University, Cambridge, MA, USA; MNA, Museum of Northern Arizona, Flagstaff, AZ, USA; NMMNH, New Mexico Museum of Natural History and Science, Albuquerque, NM, USA; QG, Natural History Museum of Zimbabwe, Bulawayo, Zimbabwe; SMP VP, State Museum of Pennsylvania, Harrisburg, PA, USA; TMP, Royal Tyrrell Museum of Paleontology, Drumheller, Alberta, Canada; UCM, University of Colorado Museum of Natural History, Boulder, CO, USA; UCMP, University of California Museum of Paleontology, Berkeley, CA, USA; UMNH VP, Utah Museum of Natural History, Salt Lake City, UT, USA; YPM, Yale Peabody Museum of Natural History, New Haven, CT, USA.

Methods

Taxonomic justification and nomenclature

The generic name of the Zimbabwean coelophysoid theropod *'Syntarsus' rhodesiensis* (Raath, 1969) has been changed several times: when the name *Syntarsus* was found to be previously occupied by a beetle genus, and therefore taxonomically invalid to apply to a dinosaur, *'S.' rhodesiensis* was placed in the genus *Megapnosaurus* ('big dead reptile'; Ivie et al. 2001). Bristowe & Raath (2004) synonymized *Megapnosaurus* with *Coelophysis*, making the formal name of the Zimbabwean coelophysoid *Coelophysis rhodesiensis*, because *Coelophysis* had taxonomic priority. However, recent phylogenetic analyses have placed *Coelophysis rhodesiensis* as more closely related to *Camposaurus arizonensis* than to *Coelophysis bauri* (Ezcurra & Brusatte, 2011; You et al. 2014; Martill et al. 2016), making the genus *Coelophysis* paraphyletic and therefore taxonomically undesirable. Because synonymizing *Camposaurus* with *Coelophysis* to resolve this problem could simply result in a similar taxonomic problem arising in the future with other analyses and more taxa, I here follow Ivie et al. (2001) in referring to the Zimbabwean coelophysoid theropod as *Megapnosaurus rhodesiensis*. Because the generic name of the Early Jurassic coelophysoid *'Syntarsus' kayentakatae* (Rowe, 1989) has not been formally changed to either *Coelophysis* or *Megapnosaurus* (nor should it be, because this would render either generic name used non-monophyletic; Ezcurra & Brusatte, 2011; You et al. 2014; Martill et al. 2016), I refer to this taxon with the generic name in quotes. I follow the definition of Coelophysoidea Sereno et al. (2005) as the clade that includes all taxa that share a more recent common ancestor with *Coelophysis bauri* than with *Allosaurus fragilis*.

One individual of *C. bauri* used in this study (TMP 1984.063.0001, #1) has previously been identified as belonging to the non-dinosaurian dinosauriform taxon *Eucoelophysis baldwini* based on the morphology of the proximal end of the femur (Rinehart et al. 2009). However, the morphology of the anterior (= 'lesser') trochanter, lacking a trochanteric shelf, is that of a morphologically immature individual of *C. bauri*, *M. rhodesiensis* (character 14, this study), as well as immature individuals of *Asilisaurus kongwe* (Griffin & Nesbitt, 2016a) and *Silesaurus opolensis* (Piechowski et al. 2014) and is therefore not diagnostic of *E. baldwini*. The morphology of the dorsolateral trochanter (= 'anterolateral trochanter' of Rinehart et al. 2009) is similarly indicative of an immature individual of *C. bauri*, *M. rhodesiensis* (character 16, this study), and *S. opolensis* (Piechowski et al. 2014), and is also not diagnostic. Additionally, the femoral head of this specimen is partially covered by matrix in the acetabulum, which causes the illusion that the 'notch' on the femoral head that characterizes *Eucoelophysis* and other silesaurids,

but not dinosaurs (Nesbitt et al. 2010; Nesbitt, 2011), is present in this specimen. Based on the presence of clear dinosaurian synapomorphies (e.g. 'perforate' acetabulum, Gauthier, 1984; Langer & Benton, 2006; Nesbitt, 2011; cnemial crest arcs anterolaterally, Nesbitt, 2011) I consider this specimen to be *C. bauri*. The individuals sampled from both taxa are from geographically and temporally constrained populations (see discussion in Griffin & Nesbitt, 2016b; Supporting Information), and in the case of *C. bauri*, were probably buried together in only one to two events (Schwartz & Gillette, 1994).

Measurements and scoring ontogenetic characters

I measured dimensions of long bones, pelves, and tarsal elements with a Cen-Tech 6-inch digital caliper, and if the dimension in question was too large for this caliper to measure, I took multiple measurements in the same dimension and added them together. When this was not possible I used a millimeter-graduated measuring tape to measure the element in question. To compare the sizes of different specimens with non-overlapping elements, I used linear regressions to estimate femoral length for all specimens, thereby standardizing all specimen sizes (Supporting Information Table S1–S3). In a few cases, a statistically significant regression between a certain measurement (e.g. the maximum width of the distal end of the tibia) and femoral length could not be constructed because of a low sample size, and in these cases I used a linear regression to estimate the length of another element that did have a significant regression with femur length (e.g. tibia length). Although this adds another step of uncertainty to the final estimated femur length, it was only necessary for a few, highly incomplete specimens (Supporting Information Data S1–S12). Because the postcranial anatomy and proportions of *C. bauri* and *Megapnosaurus rhodesiensis* are so similar (Colbert, 1989; Bristowe & Raath, 2004), I used measurements from both taxa to construct these linear regressions. To test whether the femoral lengths of *C. bauri* and *M. rhodesiensis* were unimodal, I used the diptest package in R (Maechler, 2015); in neither taxon are the femoral sizes in the studied population multimodal (*C. bauri*, $P = 0.9659$; *M. rhodesiensis*, $P = 0.6758$). I used the Shapiro–Wilk normality test to determine whether the femoral lengths of *C. bauri* and *M. rhodesiensis* were normally distributed. Whereas the femoral lengths of *M. rhodesiensis* possessed normal distribution ($P = 0.2278$), those of *C. bauri* were non-normally distributed ($P = 5.892 \times 10^{-7}$). To assess whether a there existed a statistically significant difference in femoral size between the two taxa, I used a Mann–Whitney-Wilcoxon test in R, which unlike a *t*-test does not require normal distributions of the samples being assessed. The known individuals of *M. rhodesiensis* are larger on average than those of *C. bauri* ($P = 2.2 \times 10^{-16}$).

The scoring for characters that were either present or absent (e.g. bone scars) was straightforward. Co-ossification events are not as easily scored, however, because a suture can possess varying degrees of closure, both across individuals and at different locations on the suture itself. Previous studies have utilized a three-tiered method of scoring suture closures, with the most immature state being an open suture, the intermediate state being a closed suture with a line of suture still visible, and the suture completely obliterated in the final state (Brochu, 1996; Irmis, 2007; Bailleul et al. 2016). This method of scoring is useful for specimens of extant taxa and three-dimensional well-preserved fossils because sutures can show varying states of closure depending the portion of the suture being observed; however, many specimens of *C. bauri* and *M. rhodesiensis* are incompletely preserved, and most specimens of *C. bauri* are preserved in blocks, with matrix obscuring part or most of the specimen. Further, I do not know *a priori* whether all sutures in these taxa fuse so as to completely obliterate the line of suture in their most mature state. To reduce uncertainty, I scored sutures in only two categories. I scored fusion characters as immature in both cases of a completely open suture, and a suture incompletely open so that the three-dimensional line of suture was completely visible and formed a distinct depression between the two elements. The mature state was a suture only visible as a thin line on the surface of the bone, as an incompletely obliterated line or completely obliterated. This method of scoring suture closure reduces resolution, but still accurately represents states. Additionally, this method is conservative with respect to variation in the sample, reducing variation that may have been introduced by taphonomic or methodological factors rather than biological. Because these characters are co-ossification events and due to the presence of large, ossified muscle scars, scoring these character states is less susceptible to taphonomic influence than some other features (e.g. muscle scars preserved as thin lineations). I scored characters too damaged to interpret as [?], but taphonomic signal may still influence the amount of variation interpreted for these populations, although my conservative scoring scheme and choice of characters was intended to limit this. The ontogenetic characters described here are not exhaustive, and several other ontogenetic changes in the skeleton have been reported for coelophysoid theropods (e.g. the co-ossification of the distal ends of the ischia, of various skull elements, of the pubes, and of the astragalus and the ascending process; the morphology of the medial epicondyle of the femur and of the infrapopliteal crest of the femur; Tykoski, 2005). However, I selected only those characters for which I could confidently assess character states in the largest number of individuals.

Ontogenetic sequence analysis

Ontogenetic sequence analysis (OSA) is a size-independent, parsimony-based method of reconstructing all equally parsimonious developmental sequences with all semaphoronts (i.e. discrete morphological ontogenetic stages in a taxon, Hennig, 1966) of discrete ontogenetic characters within a population (Colbert & Rowe, 2008). OSA allows for the testing and quantification of intraspecific variation in growth patterns (Morris, 2013) and is therefore ideal to reconstruct growth patterns in *C. bauri* and *M. rhodesiensis*, which have been previously reported to possess a high degree of variability in the presence of morphological characters (Raath, 1977, 1990; Colbert, 1989, 1990; Griffin & Nesbitt, 2016b). To summarize the method, which follows Colbert & Rowe (2008): NEXUS files of irreversible developmental characters are constructed, with specimens as operational taxonomic units (OTUs). Then, a parsimony-based cladistics program (e.g. PAUP*) is used to optimize these characters onto trees, which are then used to construct a reticulating diagram showing all equally parsimonious developmental sequences in the sample. To make all sequences link the least mature semaphoront with the most mature, this analysis is run twice: the first time with the most immature semaphoront as the outgroup, and the second with the most mature semaphoront as the outgroup and character coding reversed. The trees returned from both analyses are used to construct a single reticulating diagram (e.g. Fig. 14). Because size and morphological maturity appear to be somewhat disjunctive in early theropods (e.g. Raath, 1990; Griffin & Nesbitt, 2016b; this study) OSA is preferable to reconstructing the ontogeny of these taxa because it provides a way to reconstruct developmental sequences without utilizing the common assumption that size is

correlated with ontogenetic age and maturity. See the Supporting Information Methods S1–S2 for more details of the analyses.

I examined specimens of *C. bauri* and *M. rhodesiensis* in person to evaluate developmental character states. In OSA, immature character states are scored as [0], whereas mature character states are scored as [1], with character transitions irreversible. One character (character 2) possessed multiple, ordered, irreversible character states, and for this character the most mature state was scored as [2], with the state possessing intermediate maturity scored as [1] and the least mature state scored as [0]. Missing data were scored as [?]. I stored these data as NEXUS files (Data S1–S12). For *C. bauri*, I split the data into a femoral character dataset, a tibial and tarsal/metatarsal character dataset, and a pelvic character dataset, as well as a dataset that included all ontogenetic characters from all elements in question. Because *M. rhodesiensis* consists largely of disarticulated elements, inter-elemental comparison of growth patterns was not possible to determine with any accuracy, I split ontogenetic character data for this taxon into a femoral, a tibial-tarsal, and a pelvic dataset. Because of disarticulation, the tibial-tarsal dataset of *M. rhodesiensis* lacked the two pedal characters of the tibial and tarsal/metatarsal dataset of *C. bauri*. For all datasets I then eliminated all specimens that, because of missing data, only possessed information for a single character, because these specimens are useless for reconstructing the relative timing of developmental events. Sample sizes and numbers of characters used in these datasets can be found in Table 1. I then combined specimens with identical suites of character data into a single operational taxonomic unit (OTU). Some OTUs were redundant; that is, the suite of character data they possessed was identical with that of another OTU, but the latter OTU possessed less missing data. These redundant OTUs do not add new sequence information while simultaneously introducing uncertainty into the analysis because the parsimony program is forced to reconstruct the missing data, so I eliminated them from the initial analysis using the safe taxonomic reduction function in the Claddis package (Lloyd, 2016) in R. Because safe taxonomic reduction (Wilkinson, 1995) eliminates all redundant OTUs, this method reduces uncertainty while retaining the most informative data. To run the 'reverse' analysis with the most mature semaphoront as the outgroup, reversal of character states is necessary. For the 'reverse' NEXUS files, all characters scored as [0] were scored as [1], and vice versa. The only exception was for character 2 (number of fused sacral vertebrae), for which I reversed [0] and [2] instead. For datasets which did not contain an OTU with entirely immature or mature characters, I included an artificial OTU with completely mature or immature character states to provide outgroups (see next paragraph). However, all character states were observed in the sample, and all characters states in these artificial immature and mature outgroup OTUs were observed in specimens. The 'normal' datasets can be found in Supporting Information as well as on Morphobank (project number 2736).

Using PAUP* (v. 4.0b10, Swofford, 2003), I ran a heuristic search on each NEXUS file using a tree-bisection-reconnection algorithm for 300 replicates and adding sequences randomly. When the heuristic search was completed, I collapsed all branches with a minimum length of zero and saved all trees to a .tre file. The 'normal' dataset was run with the most immature individual as the outgroup OTU, and the 'reversed' dataset run with the most mature as the outgroup. I then visualized these trees in MACCLADE (v. 4.04, Maddison & Maddison, 2002) with the 'trace all changes' function used to see all reconstructed character transformations for all trees. This was done for all 'normal' and 'reverse' datasets, and then reticulating diagrams were constructed for each pair of datasets following standard OSA procedure (Colbert & Rowe, 2008). Although I followed the standard OSA method described by Colbert & Rowe (2008), some modifications were necessary to accommodate a dataset with a larger than normal amount of missing data, and to do so I followed the methodology described in Griffin & Nesbitt (2016b).

Table 1 Results of ontogenetic sequence analyses of *Coelophysis* and *Megapnosaurus* indicate a large amount of intraspecific variation in developmental patterns.

Coelophysis bauri	*n*	No. of characters	No. of sequences	Modal sequence weight	% all sequence weights	% all semaphoront weights
Full postcranium	174	27	136	21.82	1.31	12.6
Pelvis and sacrum	69	5	16	28.77	8.13	42
Femur	88	10	82	28.09	1.62	32
Tibia, tarsus, pes	70	8	35	30.06	3.04	42.8
Bone scars	111	15	74	44.73	1.89	40.3
Suture co-ossifications	140	12	27	34.54	4.24	25.2
Megapnosaurus rhodesiensis					34.7	89.69
Pelvis and sacrum	29	5	3	26.01	0.94	49.6
Femur	44	13	145	21.63	100	100
Tibia and tarsus	73	6	4	73	54.7	91
Humerus	18	4	2	16.34		

Additionally, because these data represent a large amount of variation in combination with a fairly large amount of missing data, one further modification to the traditional OSA methodology was required. Some specimens with a large amount of missing data nevertheless possessed suites of characters that were unique with respect to nearly all other specimens in the sample, especially in the full-body dataset of *C. bauri*. Because of this missing data, the 'normal' treatment reconstructed these specimens in sequences close to the immature outgroup in highly divergent sequences because of the unusual suite of character scores these specimens possessed. The 'reverse' treatment did the opposite, and reconstructed these specimens as being close to the mature outgroup, with missing data reconstructed as mature instead of immature character states, in highly divergent sequences. Usually, the two treatments result in all semaphoronts linked by developmental sequences which connect the immature and mature outgroup semaphoronts. Therefore, any semaphoront that is not linked to the mature semaphoront in the 'normal' treatment is linked by the 'reverse' treatment, and vice versa. However, because the same specimens were reconstructed in such different places in the reticulating diagram, and possessed

such anomalous suites of character states, they were left 'stranded' and did not form complete developmental sequences. This means that the same individuals were placed at either very immature or very mature locations, unconnected to other sequences. To complete these sequences, I manually connected the most mature semaphoront in the incomplete sequence to the most mature semaphoront in the OSA. I did the same thing for the least mature semaphoront of the incomplete sequence, connecting them to the least mature semaphoront overall. This resulted in a number of developmental sequences that were highly unresolved and possessed very low specimen frequency support weights. Reconstruction of the same specimens as closer to either the immature or mature outgroup semaphoront are both equally consistent with the data; however, to avoid inflating the amount of sequence polymorphism reconstructed in the population by including both reconstructed states of these specimens, I arbitrarily chose to eliminate the incomplete, manually reconstructed sequence close to the mature outgroup semaphoront, with the semaphoronts representing those same specimens reconstructed as close to the immature outgroup remaining in the final analysis. The 'raw' OSA diagrams and sequences can be found in Supporting Information (Supporting Information Figs. S1–S10).

Frequency support weight is a dimensionless number that represents the number of specimens (i.e. specimen support) for a single semaphoront. A specimen lends a support weight of 1 to a semaphoront if that is the only semaphoront which can represent the specimen. If, because of missing data, two semaphoronts are both equally consistent with a specimen, then each of those semaphoronts is lent a weight of 0.5 for that specimen. The combined specimen support in a semaphoront supports that semaphoronts frequency, and the developmental sequence possessing the highest combined frequency support weight – that is, the developmental sequence representing the most specimens – is the modal sequence.

Description

Descriptions of ontogenetic characters

1 Sacrum, neural spine co-ossification: (0) all neural spines separate; (1) neural spines fused into single sheet of bone (Fig. 1A).

In individuals of both *C. bauri* and *M. rhodesiensis* the neural spines can either be distinct structures or co-ossified into a single, continuous structure of five sacral neural spines. This variation in co-ossification has been suggested to be sexual dimorphic, with one sex possessing unfused sacral spines and the other fused spines (Colbert, 1989, 1990; Rinehart et al. 2009), but I follow Raath (1990) in interpreting this character as being variable through ontogeny, with unfused spines as the immature character state and spines fused into a single bony sheet as the mature state. This hypothesis is supported by the existence of individuals with intermediate character states: in one individual of *C. bauri* (AMNH FARB 7228; Fig. 1E,F), although the neural spines are fused into a single sheet, the co-ossification is

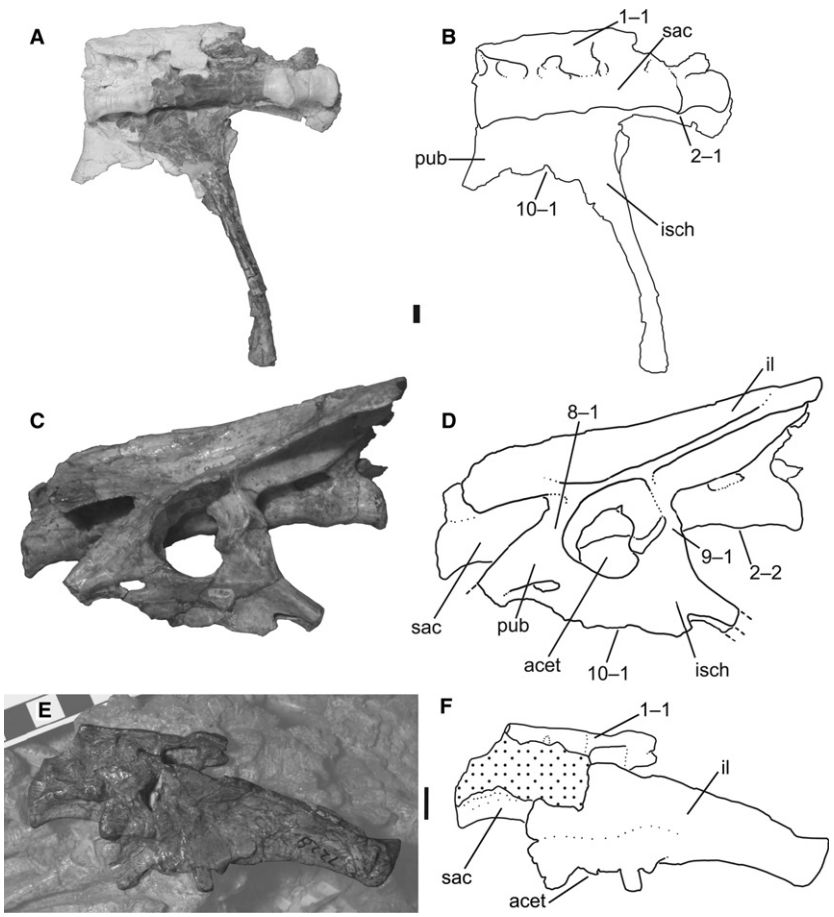

Fig. 1 Sacra and pelves of *Megapnosaurus rhodesiensis* and *Coelophysis bauri*. (A) Photograph and (B) line drawing of the sacrum, right ischium, and partial right pubis of *C. bauri* (CMNH 10971) possessing a combination of mature and immature character states, in ventrolateral view. Portions of the fossil are naturally white, not plaster. (C) Photograph and (D) line drawing of the sacrum and left pelvis of *M. rhodesiensis* (QG 1) possessing mature character states in left lateral view. (E) Photograph and (F) line drawing of the left pelvis of *C. bauri* (AMNH FARB 7228) in left lateral view, showing partially fused neural spines coded as mature. Non-target skeletal elements and matrix have been lightened in PHOTOSHOP to highlight the ilium and sacrum. Scale bars: 1 cm. acet, acetabulum; il, ilium; isch, ischium; pub, pubis; sac, sacrum.

relatively incomplete with respect to other individuals, and on the dorsal edge of the structure the individual neural spines are discernible. I scored all individuals with five fused sacral neural spines as [1], even if they were less completely fused than others, because this minor variation in individuals with fused spines was only discernible in exceptionally well-preserved individuals, whereas for most individuals I was only able to determine if the spines were separate or fused together. Because I could only confidently determine the relative degree of co-ossification in a few individuals, I chose to consider co-ossification of all degrees as state [1]. Although incomplete fusion may have existed in this sample and was simply not preserved in the fossil record, this method of scoring is conservative with respect to reporting variation.

2 Sacrum, number of sacral centra co-ossified: (0) zero to three co-ossified sacral centra; (1) four co-ossified sacral centra; (2) five co-ossified sacral centra. Ordered character (Fig. 1B,D).

In most of the largest individuals of *C. bauri* and *M. rhodesiensis* the centra of the five sacral vertebrae are fused together, with the suture between centra obliterated, producing a smooth continuous surface. However, many individuals possess only four sacrals in this co-ossified structure, with the posteriormost sacral (sacral 5) remaining unfused. Some individuals of *C. bauri* possess only three fused sacrals, with four and five remaining unfused, and one individual (TMP 1984.063.0001, #1) lacks co-ossification between all centra. Because observation of the sacrum is partially obscured by the ilium in many specimens, especially those of *C. bauri*, in these specimens I was only able to determine whether the centra of sacral vertebrae 1 and 2 and sacrals 4 and 5 were co-ossified, with the articulations between sacrals 2, 3, and 4 remaining covered. Because I never observed an individual with the anterior two or posterior two sacrals fused without co-ossification between the interior sacrals, and because the position of these interior sacrals was always consistent with their being fused into a single structure, I chose to score these as fused even when the co-ossifications themselves were not visible. Therefore, an individual with observed co-ossification between sacral centra 1 and 2, and 4 and 5, was scored as [2]. An individual with co-ossification between sacrals 1 and 2, but not 4 and 5, was scored as [1]. This method of scoring this character is conservative with respect to the amount of variation in the sample because it will underestimate, rather than overestimate, intraspecific variation in the number of fused sacral centra.

Only a few individuals of *C. bauri* were scored as fully immature [0] for this character, and in two of these individuals the anterior three sacrals were co-ossified, with sacrals 4 and 5 remaining unfused to their adjacent sacral centra (AMNH FARB 7230, NMMNH P-42353). However, in TMP 1984.063.0001, #1 all articulations of sacral centra that are visible are unfused, with only the articulation between sacrals 2 and 3 obscured by the ilium. Unlike the other sacral vertebrae in this individual, sacrals 2 and 3 are roughly in life position, consistent with both their being fused, or with their simply being in proper articulation with each other. Therefore, I cannot say with certainty whether there are two fused sacrals in this individual, or none. Two specimens of *M. rhodesiensis* (QG 179; unnumbered) consisted entirely of two unfused sacrals, and these can be confidently identified as either sacrals 2 and 3 or 3 and 4 because the articulations for the sacral ribs are shared between centra (Nesbitt, 2011), justifying a score of [0]. If the hypothesized sequence of sacral co-ossification in *C. bauri* holds for *M. rhodesiensis*, this suggests that these two specimens possess no fused sacrals, because co-ossifications between sacral centra 2 and at least one adjacent centrum would be expected to be the first co-ossification event to occur following the order of co-ossification I have hypothesized above.

Co-ossification of sacral centra is a synapomorphy of Neotheropoda, with the proximal outgroups of this clade (e.g. *Herrerasaurus*, *Staurikosaurus*, *Saturnalia*) lacking this character state (Nesbitt, 2011). Sacral centra are also co-ossified in ornithischian dinosaurs, some sauropodomorphs, pterosaurs, and several pseudosuchian lineages; however, the sacral centra of the silesaurid *Silesaurus opolensis* lack co-ossification (Nesbitt, 2011), so this character state has evolved independently in multiple archosaurian lineages. A large individual of the neotheropod *Dilophosaurus wetherilli* possesses incomplete co-ossification of the two posterior sacral centra (UCMP 77270; A. Marsh, pers. comm.).

3 Scapula and coracoid, co-ossification between elements: (0) absent; (1) present (Fig. 2).

In some individuals of both *Coelophysis* and *Megapnosaurus* the scapula and coracoid have co-ossified into a single structure, the scapulocoracoid, with the line of suture either completely obliterated or so faint that the elements cannot be disassociated.

Co-ossification between the scapula and coracoid is common in the ontogeny of amniotes and is present in many reptiles, including lepidosaurs (Romer, 1956), turtles (Lee, 1996), crocodylians (e.g. Brochu, 1992), phytosaurs (Camp, 1930), silesaurids (e.g. *Asilisaurus kongwe*, NMT RB159; *Silesaurus opolensis*, Dzik, 2003), and early saurischians (e.g. *Eoraptor lunensis*, Sereno et al. 2013). Given the widespread distribution of this character across Reptilia, it may be the ancestral saurian condition to fuse the scapula and coracoid during ontogeny. Co-ossification of the scapula and coracoid is the only character I observed to be variable within a single individual: in NMMNH P-42577, the left scapulocoracoid is completely co-ossified, whereas the right scapula and coracoid are separate from each other. For this specimen, I scored this character as immature, following a preference for scoring characters as immature until the

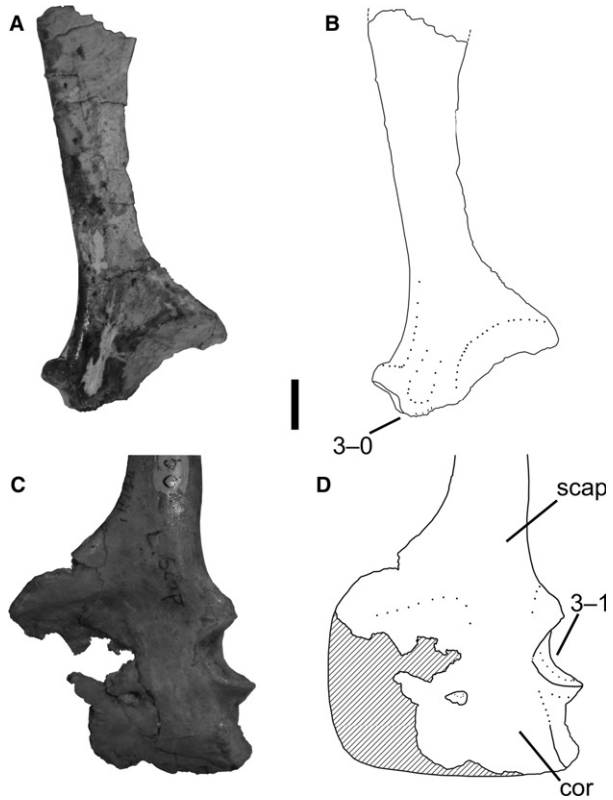

Fig. 2 Scapulae and a coracoid of *Megapnosaurus rhodesiensis* in lateral view. (A) Photograph and (B) line drawing of a right scapula (QG 528) possessing the immature character state. (C) Photograph and (D) line drawing of a left scapulocoracoid (QG 1) possessing the mature character state. Scale bar: 1 cm. cor, coracoid; scap, scapula.

mature state for that character has unambiguously been reached. Similar to *Coelophysis* and *Megapnosaurus*, whether the scapula and coracoid of *Herrerasaurus* are fused is poorly correlated with body size (Sereno, 1994), which would be expected if variation in growth patterns is the ancestral dinosaurian condition (Griffin & Nesbitt, 2016b). There has even been variation in scapulocoracoid fusion reported in individuals of *Tyrannosaurus rex* of varying size. However, this variation is in the length and morphology of a visible suture: in the large individual FMNH PR2081, the suture between the two elements is visible on the lateral side, but this suture does not represent a separation between the two elements and bone is continuous through the suture (Brochu, 2003); the small individual BMR 2002.4.1 has only a faint line of suture visible over both lateral and medial surfaces (Larson, 2013). Therefore, although there is some variation in sutural morphology, using my scoring criteria (see Materials and Methods) both individuals of *T. rex* would be considered to possess co-ossified scapulae and coracoids, and this is not evidence for a level of variation on par with early dinosaurs. Increased documentation of variation in younger taxa may reveal whether this high variation in scapulocoracoid fusion is restricted to early dinosaurs.

4 Humerus, scar of origin of *m. triceps brachii caput laterale*: (0) absent; (1) present as rugose ridge (Fig. 3).

A low, rugose ridge effectively acts as the border between the deltopectoral crest and the shaft, extending distally from the proximolateral edge of the deltopectoral crest along the humeral shaft, terminating at roughly the same location that the distal portion of the deltopectoral crest joins the humeral shaft. This feature is present in some individuals of both *C. bauri* and *M. rhodesiensis* (e.g. AMNH FARB 7223; QG 1), as well as *Segisaurus halli* (Carrano et al. 2005).

The broad anterolateral face of the deltopectoral crest is the insertion of the *m. deltoideus clavicularis* in crocodylians and *Sphenodon* (Dilkes, 2000; Meers, 2003). Burch (2014) also reconstructed this face as the insertion of the m. *deltoideus clavicularis* (hypothesized to be homologous with the *m. propatagialis* in avians; Burch, 2014) in the early theropod *Tawa hallae*, with the low ridge as the origin of the M. triceps brachii caput laterale (TBL), marking the posterior margin of the *m. deltoideus clavicularis* insertion area. Given that this feature is common in theropods, early sauropodomorphs (*Saturnalia,* Langer et al. 2007), and non-dinosaurian dinosauromorphs (*Dromomeron romeri*, C. T. Griffin, pers. obs., unnumbered GR specimen) I follow Burch's (2014) hypothesis for the identification of the muscle associated with this osteological feature.

5 Humerus, scar of origin of the *m. triceps brachii caput mediale*: (0) absent; (1) present as rugose ridge (Fig. 3).

M. rhodesiensis possesses a linear, rugose ridge on the proximal, posteromedial portion of the humeral shaft that is connected at its most distal point to the origination scar of the TBL. Proximal to this point, it extends posteriorly and proximally to the same proximal level as the origin scar of the triceps brachii caput laterale, forming a 'V' shape in posterolateral view from the intersection between the two scars. I did not observe this scar (character 5) in any individual of *C. bauri*; however, the hypothesized mature state of this character is variable during ontogeny in *Megapnosaurus*, and the preservation of most individuals of *C. bauri* in blocks that only expose one side of the element in question made scoring this character problematic for the majority of individuals. Because this scar is absent in otherwise robust, mature individuals of both *C. bauri* and *'S.' kayentakatae*, I hypothesize that this character is an autapomorphy of *M. rhodesiensis* and is not present in other coelophysoids regardless of morphological maturity.

In extant crocodylians and birds, the origin of the *m. triceps brachii caput medialis* (TBM) is a wide region on the posteromedial potion of the humeral shaft, extending distally from the posteroproximal region of the humerus to cover nearly the entire humeral shaft (Burch, 2014). The proximalmost portion of the origin of this muscle is bifurcated, and I hypothesize that the rugose ridge that extends

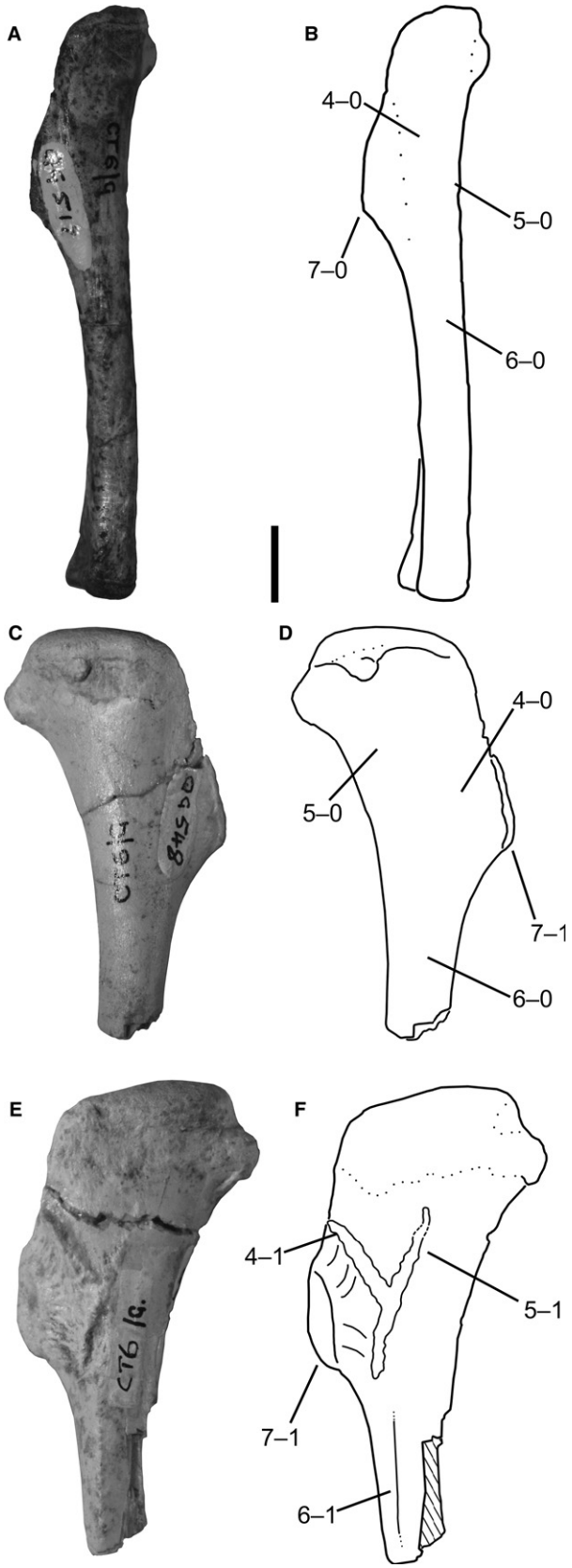

Fig. 3 Humeri of *Megapnosaurus rhodesiensis*. (A) Photograph and (B) line drawing of a left humerus (QG 517) possessing immature character states in lateral view. (C) Photograph and (D) line drawing of a right humerus (QG 548) possessing a combination of mature and immature character states in posterior view. (E) Photograph and (F) line drawing of a left humerus (QG 543) possessing mature character states in posterior view. Scale bar: 1 cm.

proximomedially away from the origin scar of the TBL is the osteological correlate for the origin of the lateral branch of the proximal region of the origin of the TBM. Although this muscle has been reconstructed in theropods to possess an origin consistent with the location of this scar (Burch, 2014), the origin of this muscle has not been previously hypothesized to correspond to a bone scar or other osteological correlate.

6 Humerus, raised lineation along posterior portion of the humeral shaft: (0) absent; (1) present (Fig. 3).

A raised proximodistally oriented lineation morphologically similar to the femoral intermuscular lines (see characters 17 and 18) is present along the posterior face of the humerus in *M. rhodesiensis*, originating just distal and posterior to the deltopectoral crest and origin scar of the TBM, and terminating halfway down the humeral shaft. This is not observed in any individuals of *C. bauri* but, like the scar for the origin of the TBM (character 5), this may be the result of sampling or preservational issues. However, similar to the origination scar for the TBM, this line is absent in otherwise robust, mature individuals of both *C. bauri* and *'S.' kayentakatae*, so I hypothesize that this character is also an autapomorphy of *M. rhodesiensis*.

The humeri of many other theropods (e.g. dromaeosaurids, troodontids, *T. hallae*) have been reported to possess a linear groove on the lateral side of the humerus posterior to the deltopectoral crest, and this has been thought to represent the insertion site of the *m. latissimus dorsi* in these taxa (Jasinoski et al. 2006; Burch, 2014). In extant crocodylians and birds the insertion of this muscle is marked by a rugose scar or tuberosity (Meers, 2003; Jasinoski et al. 2006), and in birds as a scar or long ridge (Jasinoski et al. 2006). Unlike in *Tawa*, which possesses a groove, in *M. rhodesiensis* this is a raised ridge; however, because this ridge is situated in a similar position to that reconstructed at the insertion of the *m. latissimus dorsi* for *T. hallae* (Burch, 2014: fig. 3) and *Majungasaurus cranatissimus* (Burch, 2017: fig. 3), I hypothesize that this scar is the osteological correlate for the insertion of the m. *latissimus dorsi* in *M. rhodesiensis*.

7 Humerus, deltopectoral crest: (0) gracile and mediolaterally thin; (1) robust and thick in the anterior portion (Fig. 3).

In *Coelophysis* and *Megapnosaurus* the anteriormost portion of the deltopectoral crest of the humerus possesses two morphologies, gracile and robust, analogous to the two morphologies of the fourth trochanter in these taxa (see character 23) and in *A. kongwe* (Griffin & Nesbitt, 2016a) and *Dromomeron gregorii* (Nesbitt et al. 2009a). In the gracile state (e.g. QG 517) the deltopectoral crest is smooth to the apex on the anterior portion of the crest, and is less extended anteriorly than in more mature individuals. The robust state (e.g. QG 543) possesses a large, raised rugose surface on the apex of the deltopectoral crest, similar in morphology to hypertrophied muscle scars, and because of this, the crest extends farther anteriorly.

The apex of the deltopectoral crest, along with the area immediately lateral to it, is the insertion of the *m. supracoracoideus* in crocodylians (Meers, 2003), although in birds that insertion has shifted to the posterior surface of the greater tubercle (Jasinoski et al. 2006). In reconstructing the musculature of *T. hallae*, Burch (2014) hypothesized that the apex of the deltopectoral crest remained the insertion of the *m. supracoracoideus* in this taxon, and I follow this hypothesis that the apex of the deltopectoral crest, and especially the hypertrophied ossification that is present in some individuals, is the osteological correlate of the *m. supracoracoideus* insertion.

8 Ilium and pubis, co-ossification: (0) absent; (1) present (Figs 1D, 4B, and 5).

The ilium fuses with the proximal end of the pubis in some individuals of both *C. bauri* and *M. rhodesiensis*. The suture between these two elements is completely obliterated during this co-ossification, and a slightly raised area is present at the region of the suture.

Co-ossification between the ilium and pubis, ilium and ischium (character 9), and pubis and ischium (character 10) has been recognized as an ontogenetic character within coelophysoids and other early diverging non-averostran theropods (Rowe & Gauthier, 1990; Tykoski & Rowe, 2004; Tykoski, 2005). Holtz (1994, p. 1103) found the character 'ilium fused with pubis and ischium in adults' to be a synapomorphy of Ceratosauria, a clade according to Gauthier (1984) which included coelophysoid neotheropods and other early neotheropods that are now often placed in a grade outside Averostra (Carrano & Sampson, 1999; Forster, 1999; Carrano et al. 2002; Rauhut, 2003; Wilson et al. 2003; Sereno et al. 2004). However, although *'S.' kayentakatae* is known to co-ossify its pelvic elements, *Liliensternus liliensterni* is known only from individuals with unfused pelvic elements (Tykoski, 2005), as is *Cryolophosaurus ellioti* (Smith et al. 2007), and *Gojirasaurus quayi* (UCM 47221; Carpenter, 1997) is only known from an individual possessing a completely unfused right pubis. In contrast, a large individual of *D. wetherilli* possesses a co-ossified pubis and ilium (UCMP 77270, A. Marsh, pers. comm.). Therefore, how widespread these ontogenetic characters are among early theropods is poorly constrained. Although *Ceratosaurus nasicornis* completely co-ossifies its pelvic elements (Marsh, 1884, 1892), even morphologically mature individuals of *A. fragilis* lack pelvic co-ossification (Madsen, 1976), suggesting that pelvic co-ossification may occur during ontogeny in all non-averostran neotheropods. Pelvic co-ossification is rare outside of Theropoda, with early sauropodomorphs (e.g. *Plateosaurus engelhardti*, Galton, 1990), silesaurids (*S. opolensis*, Dzik, 2003; *A. kongwe*, NMT RB159), and early saurischians (Holtz & Osmólska, 2004) lacking co-ossification of pelvic elements, although the pelvis of the dinosauriform *Marasuchus*

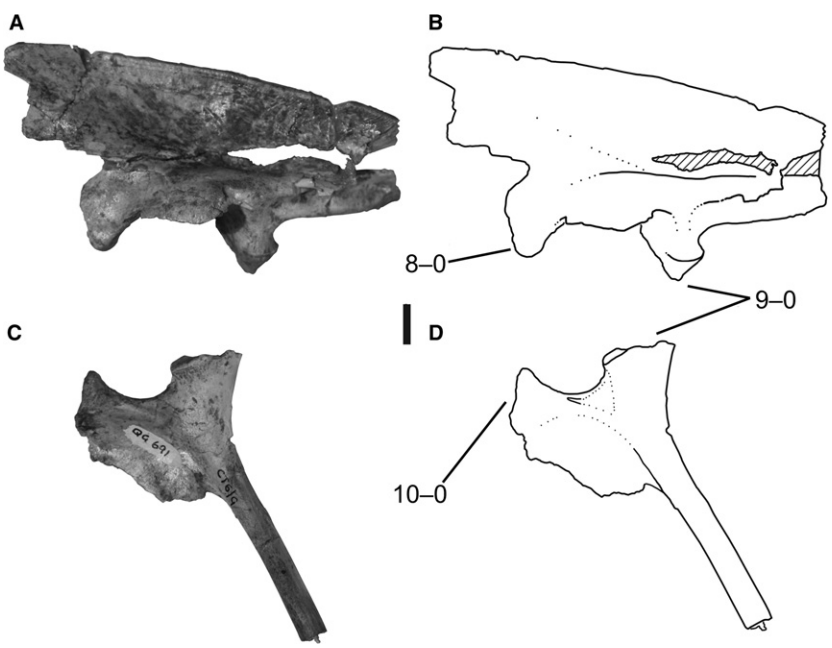

Fig. 4 Ilium and ischium of *Megapnosaurus rhodesiensis*. (A) Photograph and (B) line drawing of left ilium (QG 691) possessing immature character states in lateral view.(C) Photograph and (D) line drawing of left ischium (QG 691) possessing immature character states in lateral view. Scale bar: 1 cm.

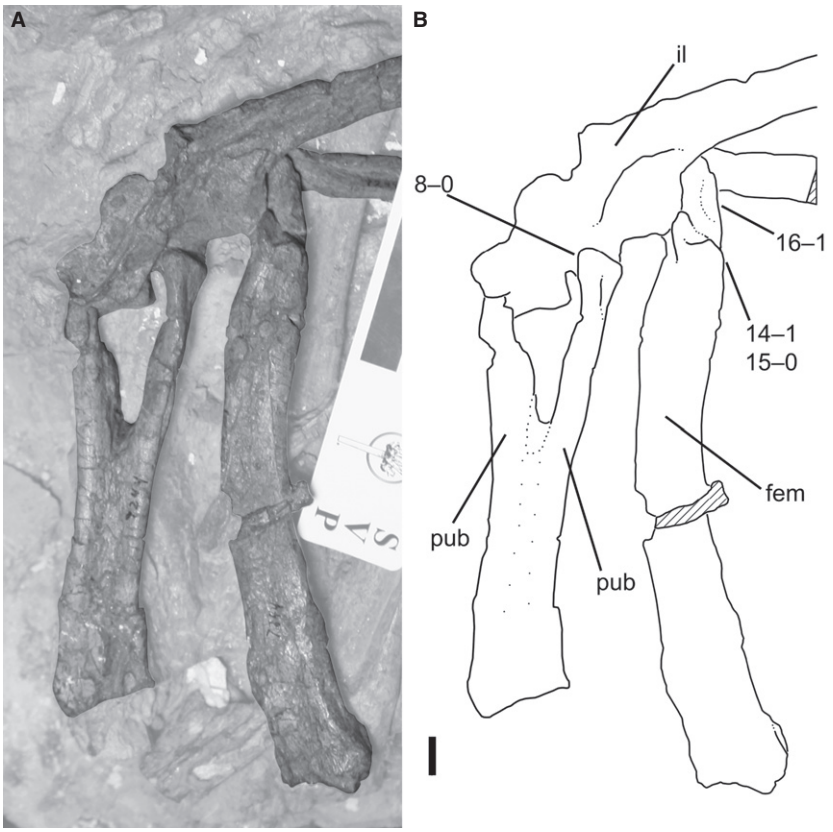

Fig. 5 (A) Photograph and (B) line drawing of articulated pubes, left ilium, and left femur of *Coelophysis bauri* (AMNH FARB 7244) in anterior view, possessing a combination of mature and immature character states. Non-target skeletal elements and matrix are lightened in Photoshop to highlight relevant skeletal elements. Scale bar: 1 cm. fem, femur; il, ilium, pub, pubis.

lilloensis is completely fused (Sereno & Arcucci, 1994). Although the distal ends of the pubes and ischia are fused in some individuals of *Coelophysis* (Colbert, 1989), I chose not to include this as an ontogenetic character because preservation made this feature difficult to assess consistently.

9 Ilium and ischium, co-ossification: (0) absent; (1) present (Figs 1D and 4B,D).

The ilium and ischium are completely co-ossified in some individuals of both *C. bauri* and *M. rhodesiensis*, and the homology of this character is discussed in conjunction with the other pelvic ontogenetic characters of the pelvis in the description of character 8.

10 Pubis and ischium, co-o-ossification: (0) absent; (1) present (Figs 1B,D and 4D).

The pubis and ischium are completely co-ossified in some individuals of both *C. bauri* and *M. rhodesiensis*. The homology of this character is discussed in conjunction with the other pelvic ontogenetic characters in the description of character 8.

11 Femur, shallow groove on proximal surface: (0) present and deep; (1) faint, and nearly absent (Fig. 6).

In many smaller or less morphologically mature individuals of *M. rhodesiensis* (e.g. QG 713, 714, 741) the proximal surface of the femur possesses a shallow groove. This groove is present between the posteromedial and anterolateral tubera in proximal aspect and extends down the middle of the proximal surface of the femur to posterodistalmost surface of the posterolateral tuber, curving medially slightly near the posterolateral depression (*sensu* Novas, 1996). This groove is so shallow as to be almost entirely absent in many larger or more robust femora, and all individuals of *C. bauri* for which this character could be scored possess this morphology.

The presence, absence, and different morphologies of a groove on the proximal surface of the femur have been used as phylogenetic character states in studies of archosaur relationships (Ezcurra, 2006, 2016; Nesbitt, 2011). Many crocodile-line archosaurs, as well as silesaurids, possess a relatively deep straight groove on the proximal surface of the femur, whereas many other pseudosuchians and avemetatarsalians possess a rounded proximal femoral surface, with no groove. Smaller individuals of the aetosaur *Typothorax coccinarum* possess a groove, whereas in larger individuals the proximal femoral surface is smooth, suggesting that this character is ontogenetically variable in this taxon (Nesbitt, 2011). Nesbitt (2011) described early-diverging neotheropods (i.e. *C. bauri*) as possessing a curved groove on the proximal surface of the femur, and it is this groove that I find to be ontogenetically variable in morphology. Because both *L. liliensterni* (HMN MB.R.2175) and the 'Padian *Coelophysis*' (UCMP 129618)

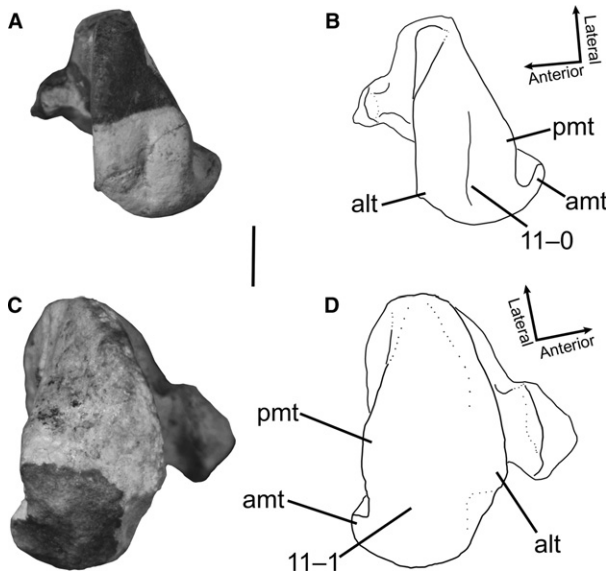

Fig. 6 Proximal ends of femora of *Megapnosaurus rhodesiensis* in proximal view. (A) Photograph and (B) line drawing of right femur (QG 174B) possessing the immature character state. (C) Photograph and (D) line drawing of left femur (QG 3A) possessing the mature character state. alt, anterolateral tuber; amt, anteromedial tuber; pmt, posteromedial tuber. Scale bar: 1 cm.

possess this groove, this is not an autapomorphy of *M. rhodesiensis*. This groove may be the osteological correlate of the extension of the cartilage cone into the proximal end of the femur (Tsai & Holliday, 2014).

12 Femur, depression on anterolateral face of proximal portion: (0) present; (1) absent (Fig. 7B).

In many smaller or less morphologically mature femora of *M. rhodesiensis* (e.g. QG 691) there is a shallow depression on the anterolateral face of the proximal portion of the femur. The edge of the depression is sharp posterior to the anterolateral tuber and just distal to the articular surface, forming a well-defined border on the anterior and proximal sides of the depression. However, the depression is poorly defined along the posterior and distal regions, and the surface of the depression grades into the normal cortical bone, making a distinct border between the depression and normal bone impossible to determine. The depression is deepest anteroproximally, nearest to the distinct edge. No femora of *C. bauri* possess this feature, even in extremely small and gracile individuals. This suggests either that all observed femora are too morphologically mature to possess the immature state of this ontogenetic character or that this character is never present in *C. bauri*.

Raath (1977, 1990) referred to this feature as a 'shallow dimple', interpreting it as a location of ligament attachment homologous with the avian teres ligament (*sensu* Cracraft, 1971). I interpret this shallow pit, along with the anterolateral scar (character 19), as an osteological correlate of the attachment of the iliofemoral ligament, which inserts

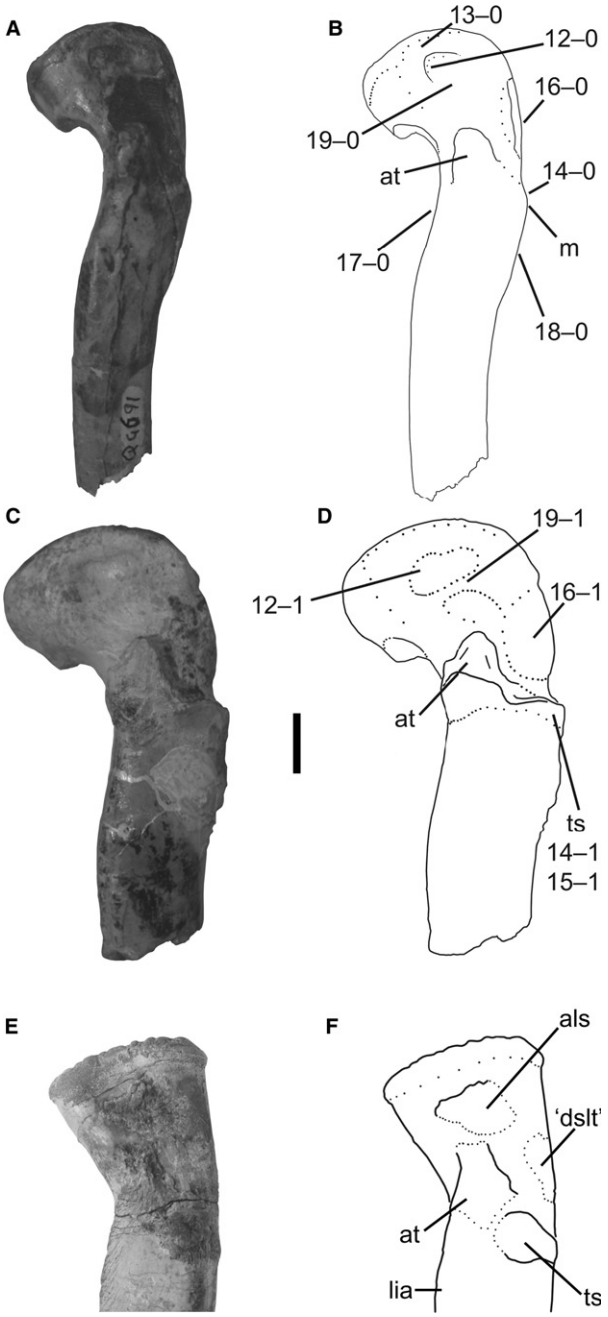

Fig. 7 Proximal ends of left femora of *Megapnosaurus rhodesiensis*, and a right femur (reversed) of *A. kongwe*, in anterolateral view. (A) Photograph and (B) line drawing of femur (QG 691) possessing immature character states. (C) Photograph and (D) line drawing of femur (QG 727) possessing mature character states. (E) Photograph and (F) line drawing of right femur (NMT RB159, reversed for comparison) to compare morphologies of scars, particularly the anterolateral scar. Scale bar: 1 cm. als, anterolateral scar; at, anterior trochanter; 'dslt', scar homologous with the dorsolateral trochanter; lia, *linea intermuscularis cranialis*; m, mound; ts, trochanteric shelf.

on the anterolateral face of the proximal end of the femur in *Alligator mississippiensis* (Tsai & Holliday, 2014). The shallow 'basin' bordered laterodistally by the anterolateral scar

makes up the majority of the insertion surface of the iliofemoral ligament (see discussion for character 19), and the sharp depression in some individuals of *M. rhodesiensis* marks the medioproximal border of this insertion area. The region bordered by these two features is roughly the same shape and relative area as the anterolateral scar of silesaurids, further suggesting that both these features represent parts of the attachment area of the iliofemoralis ligament. Because this pit is largely present in less morphologically mature individuals of *M. rhodesiensis*, and the anterolateral scar is present in mature morphs, few femora possess both structures. I have not observed this feature in its immature state in any other early theropod taxon, though this may be because this feature is present in earlier ontogenetic stages than are preserved for most other taxa. This feature, or at least its appearance at such a relatively late stage in ontogeny, may therefore be autapomorphic for *M. rhodesiensis*.

13 Femur, anterolateral edge of proximal surface extending anterolaterally: (0) absent; (1) present (Fig. 8D).

The anterolateral border of the proximal surface of the femur is dorsoventrally continuous with the anterolateral face of the femur in many less mature individuals of both *C. bauri* (e.g. TMP 1984.063.0001, #1) and *M. rhodesiensis* (e.g. QG 691), but in many robust individuals this articular edge extends anterolaterally, forming a 'lip' overhanging

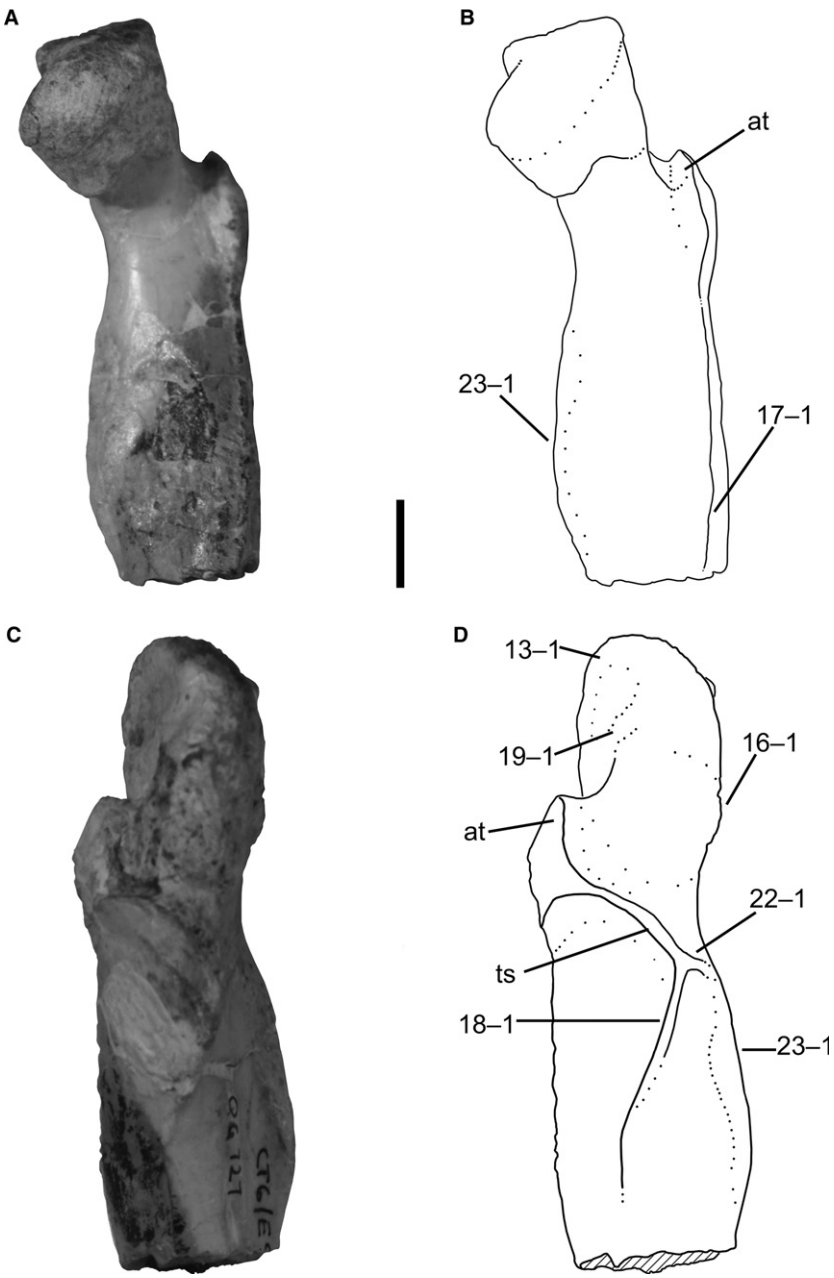

Fig. 8 Proximal end of left femur of *Megapnosaurus rhodesiensis* (QG 727) showing mature character states. (A) Photograph and (B) line drawing of femur in anteromedial view. (C) Photograph and (D) line drawing of femur in posterolateral view. Scale bar: 1 cm. at, anterior trochanter; ts, trochanteric shelf.

the anterolateral face of the femur in anteromedial or posterolateral view. Although I have observed this feature to be variable *C. bauri*, it is not nearly as variable as in *M. rhodesiensis*, and preservational issues made scoring this character much easier and more consistent in the latter taxon. Therefore, although this appears to be a feature in the ontogeny of *C. bauri* as well, I only scored this character state for *M. rhodesiensis*. I am not aware of this ontogenetic change being referred to elsewhere in the literature, so establishing any homology for this character is at present difficult.

14 Femur, trochanteric shelf: (0) absent; (1) present (Figs 5, 7, and 9F).

In *C. bauri* and *M. rhodesiensis*, the trochanteric shelf is usually a roughly horizontal rugose ledge, which forms a continuous structure with the posterodistal portion of the anterior trochanter. When present (e.g. AMNH FARB 7228), the shelf extends towards the posterior edge of the femur. The proximal part of the shelf connects abruptly with the bone surface, forming a distinct ledge, but the trochanteric shelf extends much further distally, often intersecting the bone surface at a lower angle to the lateral edge. The shelf extends laterally away from the femur, often a farther distance than its own proximodistal axis. In those specimens in which the trochanteric shelf is absent (e.g. TMP 1984.063.0001, #1; QG 691) there is a low, subtle mound, continuous with and indistinguishable from the normal subperiosteal bone surface. A similar structure exists in *T. hallae* (Nesbitt et al. 2009b; Fig. 2) some specimens of *D. wetherilli* (Welles, 1984; fig 32; A. Marsh, pers. comm. 2015) and all specimens of *A. fragilis* (Madsen, 1976; plate 50; C. T. Griffin, pers. obs.). The presence of the trochanteric shelf has been suggested to relate to ontogenetic stage in early dinosaurs and their closest relatives (Raath, 1977, 1990; Nesbitt et al. 2009a; Piechowski et al. 2014; Griffin & Nesbitt, 2016a,b).

The trochanteric shelf is the osteological correlate for the insertion of the *m. iliofemoralis* externus (= *m. iliofemoralis* in Crocodylia), and has been hypothesized to have originated in Dinosauromorpha (Hutchinson, 2001; Nesbitt et al. 2009a). This structure has been identified in non-dinosaurian dinosauromorphs (*D. gregorii*, Nesbitt et al. 2009a; *D. gigas*, Martínez et al. 2015) and dinosauriforms (*M. lilloensis*, Sereno & Arcucci, 1994; Silesauridae, Nesbitt, 2011; Piechowski et al. 2014; Griffin & Nesbitt, 2016a). The posterior portion of the trochanteric shelf has been hypothesized to correspond to the insertion of the *m. ischiotrochantericus* (Novas, 1996; Hutchinson, 2001, 2002).

The presence or absence of the trochanteric shelf is correlated with changes in the morphology of the anterior (= 'lesser') trochanter, which is present in all specimens of *C. bauri* and *M. rhodesiensis* for which the absence or presence of this feature could be observed. The anterior trochanter is the attachment site of the *m. iliotrochanteris caudalis*, and this muscle has also been hypothesized to be homologous with the *m. iliofemoralis* of crocodylians (Hutchinson, 2001). Although originally hypothesized to be a dinosauriform synapomorphy (Hutchinson, 2001), the anterior trochanter appears to be present in some non-dinosaurian dinosauromorphs (*D. gregorii*, Nesbitt et al. 2009a; potentially *D. gigas*, Martínez et al. 2015; *M. lilloensis*, Sereno & Arcucci, 1994) but is only present in a continuous structure with the trochanteric shelf. In at least some silesaurids, the anterior trochanter and trochanteric shelf are partly distinct from each other during ontogeny, but the most mature individuals usually possess both in a single continuous structure (*S. opolensis*, Dzik, 2003; Piechowski et al. 2014; *A. kongwe*, Griffin & Nesbitt, 2016a). In *Coelophysis*, the anterior trochanter usually takes two distinct forms. When the trochanteric shelf is absent (e.g. TMP 1984.063.0001, #1), the anterior trochanter is a spike-like structure oriented proximodistally, roughly twice as tall as it is anteroposteriorly wide, with the proximalmost end of the trochanter detached from the femoral surface and narrowed relative to the rest of the structure. Both the posterolateral and anteromedial faces of this structure are flattened, similar to the anterior trochanter in other dinosaurs (e.g. *T. hallae*, Nesbitt et al. 2009b; *A. fragilis*, Madsen, 1976) and non-dinosaurian dinosauriforms (e.g. *S. opolensis*, Dzik, 2003; Piechowski et al. 2014). When the trochanteric shelf is present (e.g. AMNH FARB 7228), the anterior trochanter is a rugose raised triangular surface continuous with, but distinct from, the femoral surface, and also continuous with the trochanteric shelf. The apex of the anterior trochanter, oriented anterolaterally away from the anterolateral surface of the femoral shaft, is usually continuous with the ridge of the trochanteric shelf. A few specimens (e.g. *C. bauri*, AMNH FARB 7244; *M. rhodesiensis*, QG 174) possess small and indistinct trochanteric shelves (see description of character 15), and in these specimens the anterior trochanter is morphologically similar to those in specimens completely lacking trochanteric shelves. The existence of these intermediate morphologies supports my interpretation of this variation as ontogenetic.

15 Femur, size of trochanteric shelf: (0) absent or small, does not extend past posterolateral edge of femur in anterolateral view; (1) large, extends past the posterolateral edge of femur in anterolateral view (Figs 5, 7, and 9F).

In some specimens (e.g. SMP VP 1072), the trochanteric shelf is extremely large and well developed, whereas in others (e.g. AMNH FARB 7244; QG 174) it is small, poorly developed, and does not extend posteriorly far away from the anterior trochanter in either *C. bauri* and

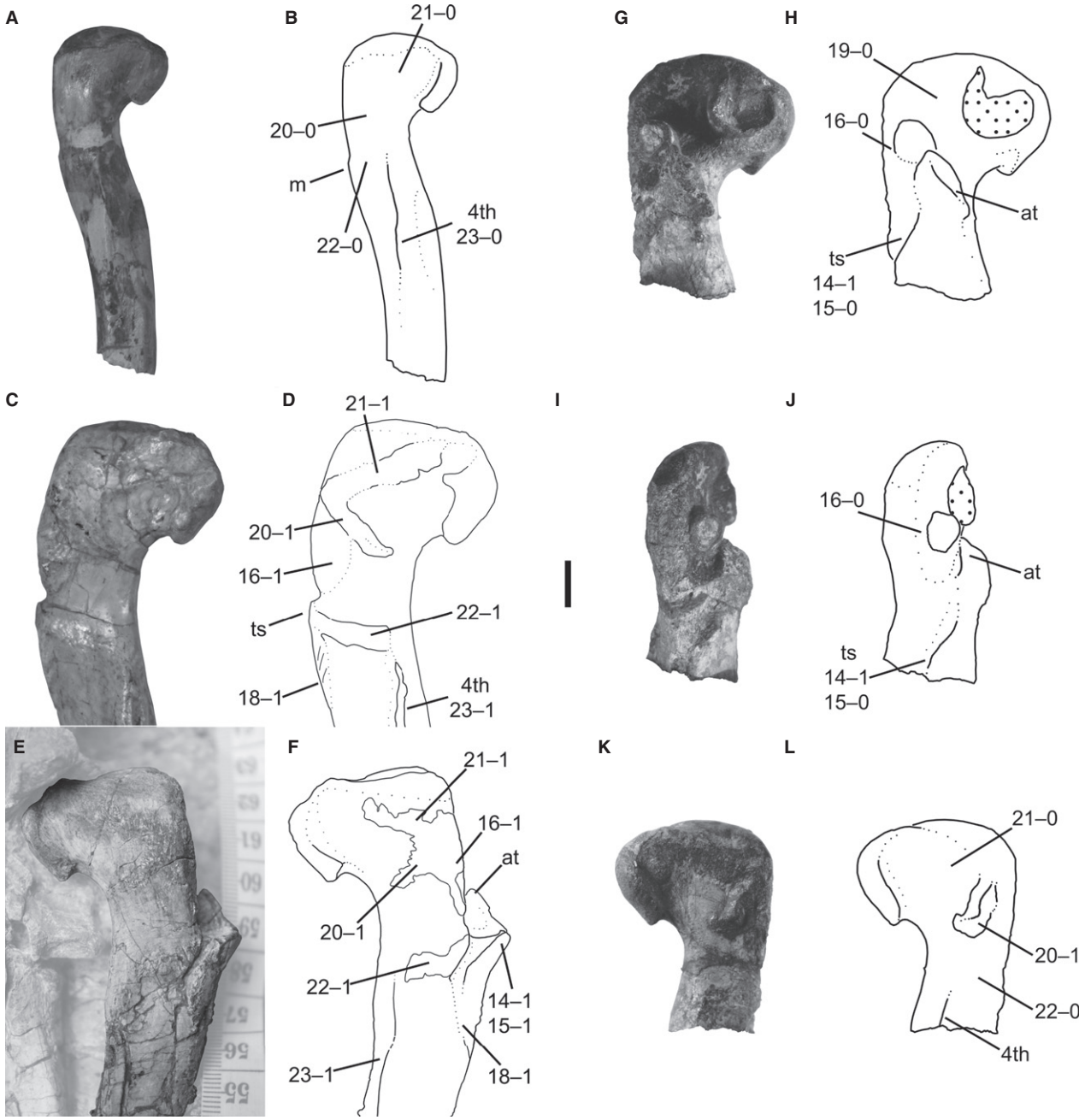

Fig. 9 Femora of *Megapnosaurus rhodesiensis* and *Coelophysis bauri* in posteromedial view. (A) Photograph and (B) line drawing of left femur of *Megapnosaurus rhodesiensis* (QG 691) possessing immature ontogenetic character states. (C) Photograph and (D) line drawing of left femur of *Megapnosaurus rhodesiensis* holotype (QG 1) possessing mature ontogenetic character states. (E) Photograph and (F) line drawing of right femur of *C. bauri* (NMMNH P-42351) possessing mature ontogenetic character states, with non-target skeletal elements and matrix lightened in Photoshop to highlight the femur. (G) Photograph and (H) line drawing of the right femur of *M. rhodesiensis* (QG 174c) possessing a combination of immature and mature character states in anterolateral view. (I) Photograph and (J) line drawing of the right femur of *M. rhodesiensis* (QG 174c) possessing a combination of immature and mature character states in posterolateral view. (K) Photograph and (L) line drawing of the right femur of *M. rhodesiensis* (QG 174c) possessing a combination of immature and mature character states in posteromedial view. Note that the protrusion near the dorsolateral trochanter of QG 174c is displaced bone. Scale bar: 1 cm. 4th, fourth trochanter; at, anterior trochanter; ts, trochanteric shelf.

M. rhodesiensis. I split the trochanteric shelf into two morphologies. Underdeveloped trochanteric shelves are those that, in anterolateral view, do not extend past the posterolateral edge of the femur but instead are confined to the area immediately posterolateral to the anterior trochanter. Large, well-developed trochanteric shelves are

those that extend past the posterolateral edge of the femur in anterolateral view. This cut-off point (the posterolateral edge of the femur) is not arbitrary but chosen because the largest trochanteric shelves in the most mature individuals are connected with the *linea intermuscularis caudalis* (character 18) and insertion scar for the *m. caudifemoralis brevis* (character 22) (Fig. 8C,D). In the latter especially, the trochanteric shelf is unable to reach this scar if it does not extend past the edge of the femur, and so the trochanteric shelf must be large enough for the femur to possess mature character states. I scored this as a separate character from character 14 rather than a single, ordered, multistate character because in some damaged specimens I was able to determine that a trochanteric shelf was present, but was unable to determine its size. These individuals were scored [1] for character 14 and [?] for character 15.

In most individuals scored as [0] for this character, the trochanteric shelf is either completely absent or is simply small, while still conforming with the description of the trochanteric shelf given in the description of character 14. However, in a few specimens the trochanteric shelf is present but underdeveloped to an unusual degree, and in these specimens the anterior trochanter normally retained the morphology only in specimens completely lacking a trochanteric shelf. These intermediate morphologies support this character as ontogenetically variable, because a shelf that is present but still developing would be expected for such a feature. Oddly, these underdeveloped shelves have differing morphologies, with some located further away from the anterior trochanter, with a gap between the two structure (AMNH FARB 7244), and others appearing to be posterolateral outgrowths of the anterior trochanter (QG 174c), suggesting that the way in which the trochanteric shelf develops might itself be variable.

16 Femur, dorsolateral trochanter: (0) ridge-like; (1) mound-like, ossified on to femur (Figs 5, 7, 8D, and 9D,F)

In *C. bauri* and *M. rhodesiensis* the dorsolateral trochanter is present in two morphologies. One morphology (e.g. QG 169) is the classic flange-like structure that is normally described as a dorsolateral trochanter in other taxa (see below). This flange is present on the posteriormost portion of the anterolateral face of the 'greater trochanter'. The proximal portion of the dorsolateral trochanter is relatively free from the femoral surface in this morph, but the distal portion of the dorsolateral trochanter is usually continuous with the 'greater trochanter'. The posterior surface of the dorsolateral trochanter tends to be rounded, with a flattened side facing anterolaterally. The second state of the dorsolateral trochanter is a large mound extending posterolaterally from the 'greater trochanter' and, unlike the flange-like state, is completely continuous with the femoral surface. This mound is often rugose in the most well-preserved specimens (e.g. AMNH FARB 7244), and the mound extends from the anterolateral face around to the posteromedial face of the 'greater trochanter'. Similarly, the scar hypothesized to be homologous with the dorsolateral trochanter extends from the anterolateral face to the posteromedial face of the 'greater trochanter' in *A. kongwe* (Griffin & Nesbitt, 2016a). In some specimens the dorsolateral trochanter possesses an intermediate morphology, and a small proximodistally oriented ridge extends out from a mound, although most of the flange is incorporated into the mound. I therefore hypothesize that the mound state is the result of the flange state being fully incorporated into the main body of the femur. Because of this, and because femora possessing the flange-like state of the dorsolateral trochanter tended to be smaller and less common than those with a robust dorsolateral trochanter, I hypothesize that the flange state is the immature ontogenetic state of this character, with the mound state being the mature state. Because the intermediate morphology still possesses flange-like characters and is therefore not fully mature, I scored this morphology as immature [0] as well.

The dorsolateral trochanter has been hypothesized to correspond to either the attachment point of one of the branches of the *mm. iliotrochanterici* (Rowe, 1986; Langer & Benton, 2006; *mm. iliotrochanterici* = *m. pubo-ischiofemoralis internus* 2 in crocodylians, Hutchinson, 2001) or *m. puboischiofemoralis externus* (Hutchinson, 2001), and is a derived dinosauriform character (Langer & Benton, 2006; Irmis et al. 2007; Nesbitt et al. 2010), synapomorphic for the clade Silesauridae + Dinosauria (Nesbitt, 2011). In addition to its presence in theropods, the dorsolateral trochanter has been described in early diverging ornithischians (e.g. *Lesothosaurus diagnosticus*, Sereno, 1991; *Eocursor parvus*, Butler, 2010) and saurischians (e.g. *Herrerasaurus ischigualastensis*, Novas, 1993; fig. 7; *Saturnalia tupiniquim*, Langer, 2003), as well as several silesaurids (*Sacisaurus agudoensis*, Ferigolo & Langer, 2006; Langer & Ferigolo, 2013; *Eucoelophysis baldwini,* Nesbitt et al. 2007; *S. opolensis*, Nesbitt, 2011; an unnamed silesaurid, TMM 31100-1303, Griffin & Nesbitt, 2016a). The dorsolateral trochanter is absent in the smallest specimens of *S. opolensis*, leading Nesbitt et al. (2007) and Piechowski et al. (2014) to consider its presence and morphology related to morphological maturity. The Middle Triassic silesaurid *A. kongwe* has been reported to possess a thin scar corresponding to the location of the dorsolateral trochanter in other silesaurids (Griffin & Nesbitt, 2016a), although all specimens referable to *A. kongwe* lack the distinct flange-like dorsolateral trochanter present in other members of this clade. Additionally, the presence of this scar is variable among femoral specimens of *A. kongwe*, which lead Griffin & Nesbitt (2016a) to follow others (Nesbitt et al. 2007; Piechowski et al. 2014) in considering the morphology of the dorsolateral trochanter to be an ontogenetically variable character.

Ancestrally, avian-line archosaurs possessed three branches of the *puboischiofemoralis externus* (PIFE 1, 2, and

3), but along the line to Neornithes, PIFE 1 and 3 were lost or strongly reduced, leaving PIFE 2 (= *m. obturatorius medialis*, OM) as the main insertion in this group (Hutchinson, 2001). The PIFE muscles, or their avian homologues, have been reconstructed to insert on the lateral surface of the 'greater trochanter' in dinosaurs (Hutchinson, 2001; Carrano & Hutchinson, 2002), and this is conserved in neornithines. I follow Hutchinson (2001) in his hypothesis that the dorsolateral trochanter is the osteological correlate of the PIFE musculature insertion.

17 Femur, *linea intermuscularis cranialis*: (0) absent; (1) present (Figs 7B and 8B).

The *linea intermuscularis cranialis* is a thin, raised proximodistally oriented lineation on the anterior or anterolateral face of the femoral shaft, created from the intersection of the *m. femorotibialis externus* and *m. femorotibialis internus* (Crocodylia, = *m. femorotibialis lateralis, mm. femorotibialis medialis* and *intermedius* in Aves; Hutchinson, 2001), and is considered to be derived for archosaurs (Hutchinson, 2001). In *C. bauri* and *M. rhodesiensis*, the *linea intermuscularis cranialis* connects to the anterodistal edge of the anterior trochanter (usually in the robust state that also possesses a trochanteric shelf) and extends distally to roughly halfway down the shaft of the femur before terminating. The presence of this character has been noted to be variable in both extinct (Nesbitt et al. 2009a; Griffin & Nesbitt, 2016a,b) and extant (Tumarkin-Deratzian et al. 2006, 2007; Griffin & Nesbitt, 2016b) archosaurs.

18 Femur, *linea intermuscularis caudalis*: (0) absent; (1) present (Figs 7B, 8D, and 9D,F).

Like the morphologically similar *linea intermuscularis cranialis*, the *linea intermuscularis caudalis* is an archosaur synapomorphy, and is a lineation formed at the border between muscles; in this case the *m. femorotibialis externus* and *m. adductor femoris* 1 & 2 (Crocodylia; = avian *m. femorotibialis lateralis* and *mm. puboischiofemorales medialis* and *lateralis*, respectively, Hutchinson, 2001; the *m. adductor femoris* 1 & 2 has been hypothesized to be homologous with the *m. pubo-ischio-trochantericus* in *Sphenodon*, Schachner et al. 2011). The *linea intermuscularis caudalis* usually extends down the posterior face of the femoral shaft (Hutchinson, 2001); in *C. bauri* and *M. rhodesiensis* it extends from the posterior edge of the trochanteric shelf down about two-thirds of the femoral shaft, and so extends further distally than the *linea intermuscularis cranialis*. Like character 17, the presence of the *linea intermuscularis caudalis* has been noted to be variable in ontogeny in both extinct (Nesbitt et al. 2009a; Griffin & Nesbitt, 2016a,b) and extant (Tumarkin-Deratzian et al. 2006, 2007) archosaurs.

19 Femur, 'anterolateral scar': (0) absent; (1) present (Figs 7D and 8D).

In femora of both *C. bauri* and *M. rhodesiensis* there is a thin, raised, mediolaterally oriented linear scar across the anterolateral face of the proximal part of the femur, proximal to the anterior trochanter. This scar is proximodistally widest at its lateral edge, where is merges with the posterolateral end of the 'greater trochanter' proximal to the dorsolateral trochanter, but as it trends medially it becomes proximodistally narrower and more linear. This scar usually intersects the distal part of the anterolateral tuber at its proximodistal midpoint. Because the area directly proximal to the ridge is depressed relative to the ridge itself, shallow 'basins' (distinct from character 12) are formed between this scar and the proximal surface of the femur in anterolateral aspect, as well as between this scar and the anterior trochanter (Fig. 7D). In *C. bauri*, this ridge is usually more distal than in *M. rhodesiensis*, resulting in the two 'basins' in *M. rhodesiensis* appearing to be roughly equal in area. In those individuals where the scar does not reach medially enough to intersect with the anterolateral tuber (e.g. QG 733), there appears to be a single 'basin', into which the scar extends laterally.

In at least some silesaurids, the anterolateral scar (= 'dorsolateral ossification', Piechowski et al. 2014) is a raised, round feature on the anterolateral face of the femoral head consisting of coarse bone fibres (Fig. 7E,F), and is hypothesized to have been variable in ontogeny (*S. opolensis*, Piechowski et al. 2014; *A. kongwe*, Griffin & Nesbitt, 2016a; the anterolateral scar is also present in the unnamed Otis Chalk silesaurid, Griffin & Nesbitt, 2016a). Because this feature is not known from any extant reptile, homologizing this structure with attachments for known muscles or ligaments is difficult. Piechowski et al. (2014) suggested that this structure is an ossified extension of the dorsolateral trochanter, because the two structures are closely associated or even continuous in *S. opolensis*. Rowe (1989: fig. 4) identified this feature as an 'insertion scar for joint capsule' in *'Syntarsus' kayentakatae* Griffin & Nesbitt (2016a) hypothesized that this structure is the insertion of the iliofemoral ligament (= pubofemoral ligament of Aves, Tsai & Holliday, 2014), citing the similar location between this insertion site in the femur of *A. mississippiensis* (Tsai & Holliday, 2014) and the anterolateral trochanter of *A. kongwe*. Given that the dorsolateral trochanter and anterolateral scar are closely associated but usually separate in all silesaurids for which it has been described, I follow Griffin & Nesbitt (2016a) in not considering this scar to be an extension of the dorsolateral trochanter in silesaurids, but a separate structure.

Although the location of this femoral scar and the anterolateral scar of silesaurids is similar, the two have differing shapes. The scar described in *C. bauri* and *M. rhodesiensis* is linear, ossified, and continuous with the cortical bone, whereas the anterolateral scar of silesaurids is a less well-attached, fibrous round structure that takes up a proportionally larger area of the anterolateral face of the

femur (Griffin & Nesbitt, 2016a). However, similar to the anterolateral scar of some silesaurids, including a few individuals of *S. opolensis* (Piechowski et al. 2014) this scar in *C. bauri* and *M. rhodesiensis* connects with the posterolateral edge of the femur, at the proximal region of the dorsolateral trochanter. A similar scar with an 'intermediate' morphology has been reported (Novas, 1993; fig. 7B) in *H. ischigualastensis*: instead of a lineation across the anterolateral face of the proximal end of the femur, in *H. ischigualastensis* the scar retains a disc-like or semicircular morphology. However, this scar is shifted laterally relative to the silesaurid condition to a position on the anterolateral face of the femur similar to that in *C. bauri* and *M. rhodesiensis*, with the wide edge of the scar continuing into the posterolateral edge of the 'greater trochanter'. Therefore, I hypothesize that this linear scar in *C. bauri* and *M. rhodesiensis*, the semicircular scar in *H. ischigualastensis*, and the anterolateral scar of silesaurids are all homologous, and I use the term 'anterolateral scar' when referring to these structures. The linear morphology of the anterolateral scar in coelophysoids may be an osteological correlate of the distal edge of the attachment of the iliofemoralis ligament, as opposed to the condition in silesaurids (and possibly *Herrerasaurus*) where the entire attachment appears to be ossified. If this is the case, then the 'basin' proximal to the anterolateral scar may take up the majority of the area of insertion of the iliofemoralis ligament, a hypothesis supported by the presence of a sharp, shallow depression in this region in *M. rhodesiensis* (see character 12).

20 Femur, 'obturator ridge' (*sensu* Raath, 1977): (0) absent; (1) present (Fig. 9).

The presence of a rounded elongate tubercle on the posteromedial face of the 'greater trochanter', identified by Raath (1977, 1990) as the 'obturator ridge', is variable in femora of *C. bauri* and *M. rhodesiensis*. In some exceptionally preserved specimens of *C. bauri* this scar has a rugose texture, and in those individuals of *M. rhodesiensis* and *C. bauri* lacking this feature, thin lineations marking the muscle attachment are often present on the cortical surface. The ridge extends anteriorly and slightly distally from the posterolateral edge of the 'greater trochanter' (directly medial to the dorsolateral trochanter) across the posteromedial face of the proximal part of the femur, terminating on the medial part of the femoral neck distal to the femoral head. This scar is probably homologous with the 'posterior portion of the dorsolateral trochanter' in *A. kongwe* (Griffin & Nesbitt, 2016a), the presence of which is also variable in ontogeny.

This tubercle in *M. rhodesiensis* has been hypothesized to be the insertion of a portion of the *mm. puboischiofemoralis externi* (PIFE; Raath, 1977), which, given this muscle complex's hypothesized homology with lepidosaurian muscles (*m. pubofemoralis pars ventralis, m. ischiofemoralis anterior,* and *m. ischiofemoralis posterior*, Schachner et al. 2011) is ancestral for all crown saurians. The three heads of the PIFE musculature in crocodylians have been hypothesized to be homologous with the *mm. obturatorius medialis* (OM) *et lateralis* (OL) of birds (Hutchinson, 2001). Scars for the insertion of the PIFE or its homologues have been identified in many pseudosuchian archosaurs (e.g. 'rauisuchians', Dutuit, 1979; crocodylomorphs, Walker, 1970; Crush, 1984; Hutchinson, 2001; extant crocodylians, Hutchinson, 2001; Schachner et al. 2011) as well as avemetatarsalians (e.g. pterosaurs, sauropodomorphs, early saurischians, Hutchinson, 2001; theropods, Andrews, 1921; Raath, 1977; Martill et al. 2000; neornithines, Ballman, 1969; Hutchinson, 2001). In birds, a scar, ridge or groove, known as the 'obturator ridge', marks insertion of the OM. Therefore, based on the location of this scar on the distal part of the 'greater trochanter', this may be the osteological correlate of part of the PIFE. However, given that in most extant archosaurs the branches of the PIFE musculature share a single insertion on the lateral surface of the 'greater trochanter', extending onto the posterolateral or posterior surface in only some extant archosaurs (Hutchinson, 2001), the anterior extent of this scar along the posteromedial face of the proximal end of the femur suggests that a different muscle(s), if present, may have inserted on the 'obturator ridge'.

21 Femur, scar proximal to 'obturator ridge': (0) absent; (1) present (Fig. 9).

A ridge extends distolaterally from the lateral portion of the posteromedial tuber across the *facies articularis antitrochanterica* to the posterolateral edge of the 'greater trochanter', converging with the lateral portion of the 'obturator ridge', in some individuals of both *C. bauri* and *M. rhodesiensis*. This scar is similar in morphology to the 'obturator ridge' but is usually not as prominent (Fig. 9C–F). Although the affinities of this scar and the 'obturator ridge' are unclear, they are physically separated and do not always appear simultaneously in ontogeny (Fig. 9), and I hypothesize that they are distinct structures. However, even if they are formed from the same muscle(s) or connective tissue, because they are distinct in ontogeny they may be scored separately for the purposes of OSA.

22 Femur, insertion scar of caudifemoralis brevis: (0) absent; (1) present (Figs 8D and 9).

A low, rugose, ridged scar connects posterolaterally to the posterior part of the trochanteric shelf and proximal part of the *linea intermuscularis caudalis* (or where these features would be in more immature individuals), extending to the proximal portion of the fourth trochanter in *C. bauri* and *M. rhodesiensis*. In well-preserved specimens that lack this feature (e.g. QG 169), small lineations are present on the surface of the cortical bone in this region. The presence of this scar is variable in the ontogeny of *A. kongwe* (Griffin & Nesbitt, 2016a).

This ridge is the insertion scar of the caudifemoralis brevis (CFB; = *caudifemoralis pars pelvica* in Aves, Hutchinson, 2001), which inserts slightly proximal and lateral to the insertion of the *caudifemoralis longus* (CFL; the insertion of which the fourth trochanter is the osteological correlate) in extant archosaurs (Hutchinson, 2001). Like the CFL, the CFB is present in crown group saurians (Hutchinson, 2001; Schachner et al. 2011).

23 Femur, fourth trochanter: (0) gracile and thin; (1) robust and thickened in the posteromedial portion of the apex of the trochanter (Fig. 9).

Analogous to the deltopectoral crest of the humerus (character 7), the fourth trochanter of the femur is present in all individuals of *C. bauri* and *M. rhodesiensis* with either gracile or robust morphology. In the gracile state (e.g. QG 174 B; MCZ 4332) the superficial apex, which is oriented proximodistally along almost the entirety of the fourth trochanter and gives the trochanter its distinctive bladed appearance, lacks scarring and a rugose texture. In contrast, the superficial apex ('blade') of the robust state of the fourth trochanter (e.g. NMMNH P-425386) is anteroposteriorly thicker and in well-preserved individuals possesses a relatively more rugose texture. Because this gracile/robust morphology extends along the proximodistal length of the fourth trochanter, this character can be scored even when only a small portion of the fourth trochanter has been preserved. The morphology of the fourth trochanter has been noted to vary during ontogeny in early bird-line archosaurs (Weishampel & Chapman, 1990; Nesbitt et al. 2009a; Griffin & Nesbitt, 2016a).

24 Tibia, tuberosity on anterior and anteromedial portion of the cnemial crest: (0) absent; (1) present (Fig. 10).

Both *Coelophysis* and *Megapnosaurus*, as well as *'S.' kayentakatae*, possess a low tuberosity on the anterior and anteromedial portion of the cnemial crest of the proximal part of the tibia. This ossified muscle scar, a low rugose mound extending anteriorly from the distal three-quarters of the cnemial crest, can be most clearly observed in medial view. In individuals without the tuberosity, the anterior edge of the cnemial crest is straight or even slightly posteriorly concave; those possessing this feature have rugose and more well-developed cnemial crests that extend further anteriorly.

Raath (1977, 1990) mentioned this scar in his description of *M. rhodesiensis*, and hypothesized that the muscles of the triceps femoris insert here. In *A. mississippiensis* the triceps femoris consists of the *m. iliotibialis* 1 (= *m. iliotibialis cranialis*, Aves), 2 and 3 (= *m. iliotibialis lateralis*, Aves), *m. ambiens, mm. femorotibialis externus* (= *m. femorotibialis lateralis*, Aves) and internus (= *mm. femorotibialis intermedius medialis*, Aves; all homology hypotheses from Carrano & Hutchinson, 2002). Given that these muscles insert

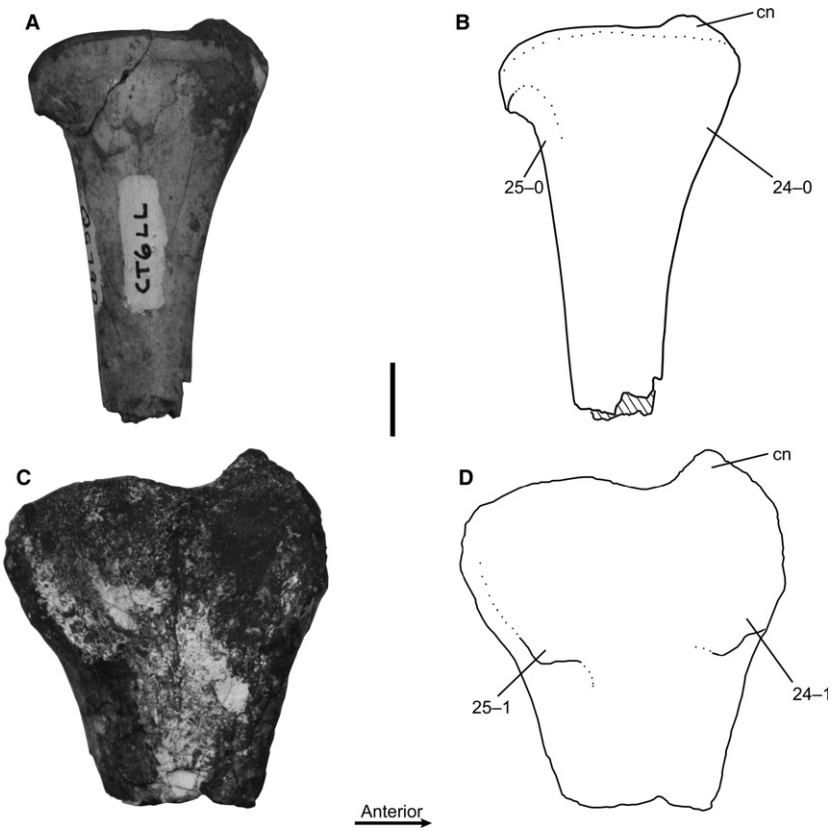

Fig. 10 Proximal ends of left tibiae of *Megapnosaurus rhodesiensis* in medial view. (A) Photograph and (B) line drawing of tibia (QG 790) possessing immature character states. (A) Photograph and (B) line drawing of tibia (QG 800) possessing mature character states. Scale bar: 1 cm. cn, cnemial crest.

on the anteroproximal part of the tibia in *A. mississippiensis*, the anterior portion of the cnemial crest in extant birds, and have been reconstructed to insert on the anterior portion of the cnemial crest in *T. rex* (Carrano & Hutchinson, 2002; Hutchinson et al. 2005), I hypothesize that this tuberosity on the cnemial crest of coelophysoids is the osteological correlate of the insertion of the *triceps femoris* group.

25 Tibia, scar on the posterior portion of the medial surface of the proximal end of the tibia: (0) absent; (1) present (Fig. 10).

Both *C. bauri* and *M. rhodesiensis* possess a scar on the posterior portion of the medial surface of the proximal end of the tibia. This rugose area, slightly raised from the surrounding bone, is most clearly visible in medial view and is morphologically similar to the mound on the cnemial crest (character 24), although it is less prominent. A rugose area in a similar location on the tibia has been suggested to represent the insertion of the *m. flexor tibialis internus* 3 (FTI3; = avian *m. flexor cruris medialis*) and *m. flexor tibialis externus* (FTE; = avian *m. flexor cruris lateralis pars pelvica*) in *T. rex* (Carrano & Hutchinson, 2002; Hutchinson et al. 2005). The FTI3 and FTE share a tendon for insertion in extant archosaurs, and so this scar is probably the insertion of both muscles.

26 Astragalus and calcaneum, co-ossification: (0) absent; (1) present (Fig. 11).

The astragalus and calcaneum fuse to form one continuous structure, the astragalocalcaneum, in *Coelophysis* and *Megapnosaurus,* but this co-ossification is much more common in individuals of *C. bauri*. Although in most archosaurian lineages the articulation between the astragalus and calcaneum remains free, many taxa along the line to birds fuse these elements in an astragalocalcaneum, including pterosaurs, early diverging dinosauromorphs, and the early ornithischian *Heterodontosaurus* (Nesbitt, 2011), as well as early neotheropods (Rowe & Gauthier, 1990). This co-ossification is widespread among early neotheropods, including *C. arizonensis* (Ezcurra & Brusatte, 2011), *'Syntarsus' kayentakatae* and the Shake-N-Bake taxon (Tykoski, 2005), *C. nasicornis* (Madsen & Welles, 2000), *Aucasaurus garridoi* (Coria et al. 2002), *Masiakasaurus knopfleri* (Carrano et al. 2002), and *Xenotarsosaurus bonapartei* (Martínez et al. 1986), among others. Tykoski (2005) considered this co-ossification to be variable in ontogeny, but appearing at a relatively early stage of development in early theropods. Therefore, this character could be ontogenetically informative across a wide phylogenetic range.

27 Tibia and astragalus, co-ossification: (0) absent; (1) present (Figs 11 and 12).

The tibia and astragalus fuse to form a tibiotarsus during ontogeny in several early neotheropods, including *C. bauri*

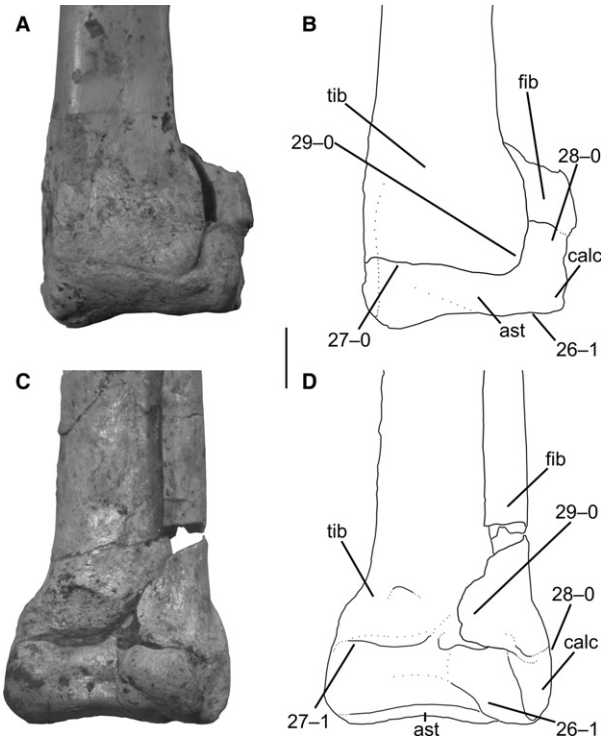

Fig. 11 Distal ends of tibiae and fibulae, with astragali and calcanea, of *Megapnosaurus rhodesiensis* possessing a combination of mature and immature character states. (A) Photograph and (B) line drawing of right tibia, fibula, astragalus, and calcaneum (QG 177) in posterior view. Note that tibia is partially co-ossified with astragalus (character 27) but is still scored as the immature state. **(**C) Photograph and (D) line drawing of left tibia, fibula, astragalus, and calcaneum (QG 805) in anterior view. Note that the distal end of the fibula is partially co-ossified with both the tibia and calcaneum (characters 28, 29), but these characters still scored as the immature states. Scale bar: 1 cm. ast, astragalus; calc, calcaneum; fib, fibula; tib, tibia.

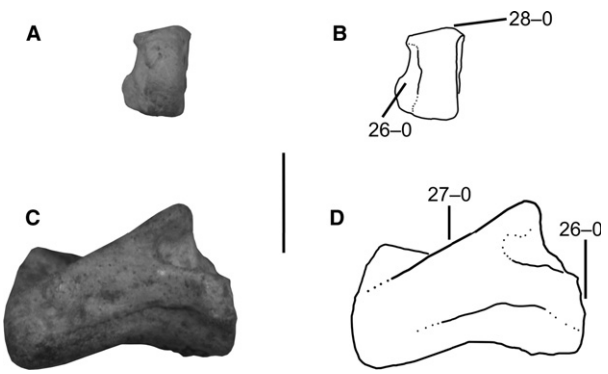

Fig. 12 Right calcaneum and left astragalus of *Megapnosaurus rhodesiensis* showing immature character states. **(**A) Photograph and (B) line drawing of calcaneum (QG 816) possessing immature character states in anterior view. (C) Photograph and (D) line drawing of astragalus (QG 820) possessing immature character states in anterior view. Scale bar: 1 cm.

and *M. rhodesiensis* (e.g. Tykoski & Rowe, 2004). However, this co-ossification is markedly different than other co-ossification events described for these taxa, including the formation of the astragalocalcaneum. In most suture co-ossifications in *C. bauri* and *M. rhodesiensis* (e.g. character 26, QG 805), the subperiosteal surfaces of the elements in question remain visible and unmodified, with the exception of the area immediately (~ 4 mm) around the suture. In contrast, the co-ossification of the tibia and astragalus in these taxa results in the posterior surface of the tibia and astragalus becoming covered by continuous rugose bone, which extends from the posteroproximal parts of the malleoli to the posteroproximal portion of the astragalus. In those individuals in which this has occurred (e.g. AMNH FARB 7247; CM 81770), no line of suture is visible in posterior aspect between the astragalus and tibia, because it is covered by the rugose layer of bone. However, this layer of bone often does not extend far around the medial sides of the astragalus or calcaneum, and a normal suture (unless obliterated) can occasionally be observed on these surfaces in individuals that possess a fused astragalus and tibia (as well as a fused fibula and tarsus; see character 28). Although co-ossification between the astragalus and tibia is visible in anterior aspect, the line of suture is never obliterated. Determining if co-ossification has occurred in an individual or there is simply tight articulation, is often difficult for individuals of *C. bauri* remaining in blocks of matrix, because only the anterior view of the tibia and tarsus is visible, and such individuals must be scored as missing data [?] for this character. One individual of *M. rhodesiensis* (QG 767) possesses the covering of rugose bone on the posterior surface of the distal end of the tibia but the astragalus has been disarticulated. However, the two elements were apparently 'fused', even though the astragalus could be broken off, because some of the rugose bone that would have covered the astragalus is still attached to the tibia extending distally from its posterodistal surface. The break along the distal surface of this rugose bone appears to be fresh, and so occurred after fossilization. This suggests that the co-ossification between the astragalus and tibia (as well as between the tarsus and fibula, and tibia and fibula; see characters 28 and 29) may not be a normal sutural co-ossification, with both elements becoming completely co-ossified and impossible to break apart without damaging the elements. If this break had not occurred, these elements would have appeared to be as completely fused as in other individuals for which this character has been scored as fused. I scored this individual (QG 767) as [1] for this character.

Although previous work has identified tibiotarsal co-ossification in *M. rhodesiensis* (Raath, 1977, 1990) and *C. bauri*, in the latter taxon Colbert (1989, 1990) suggested that this co-ossification represents individual and not ontogenetic variation because of the poor correlation between size and individuals that possess what would be considered the mature state (fused) of this character. However, body size is not a good correlate for morphological maturity in this taxon because of individual variation in ontogenetic patterns (Griffin & Nesbitt, 2016b), or in early sauropodomorphs (*P. engelhardti*, Sander & Klein, 2005) and close dinosaurian relatives (*A. kongwe*, Griffin & Nesbitt, 2016a).

Co-ossification between the tibia and astragalus is widespread among early neotheropods but is not as commonly described as astragalocalcaneum co-ossification (character 26). In addition to *M. rhodesiensis* and *C. bauri*, *C. arizonensis* (Tykoski, 2005; Ezcurra & Brusatte, 2011), *'Syntarsus' kayentakatae* (Rowe, 1986; Tykoski, 2005; this study), the Shake-N-Bake taxon (Tykoski, 2005), *C. nasicornis* (Gilmore, 1920; Madsen & Welles, 2000), *X. bonapartei* (Martínez et al. 1986), *M. knopfleri* (Carrano et al. 2002) have all been reported to possess fused tibiotarsi; however, with the exception of *'Syntarsus' kayentakatae* I have not examined these specimens in person and so cannot comment on whether the tibiotarsal co-ossification in these taxa is similar to the co-ossification described here for *C. bauri* and *M. rhodesiensis*. *Lepidus praecisio* (Nesbitt & Ezcurra, 2015), *L. liliensterni* and some individuals of *D. wetherilli* (Tykoski, 2005; the *D. wetherilli* paratype UCMP 37303 has some co-ossification of these elements, A. Marsh, pers. comm.) have all been reported to lack co-ossification between the tibia and astragalocalcaneum, either indicating that this character was lost in these taxa or that these specimens represent morphologically immature individuals.

28 Fibula and tarsus, co-ossification: (0) absent; (1) present (Fig. 11).

The fibula and tarsus fuse in a similar manner to the tibia and astragalus in *Coelophysis* and *Megapnosaurus*, except that the co-ossification between the tarsus (= astragalocalcaneum) and fibula is often more complete (that is, the line of suture is nearly or completely absent) in anterior view. The fibula is mostly articulated with the calcaneum in these taxa, but a small part of the proximolateral region of the astragalus also articulated with the fibula; co-ossification between the fibula and astragalus occurred in conjunction with all instances of fibular co-ossification with the calcaneum, and in all cases the astragalus was already co-ossified with the calcaneum when this co-ossification occurred. For these reasons, I refer to this co-ossification as between the fibula and tarsus, and not just the fibula and calcaneum, although in practice this is the same event. This character occurs in many of the same taxa as co-ossification between the tibia and astragalus (character 27).

29 Fibula and tibia, co-ossification of distal ends: (0) absent; (1) present (Fig. 11).

In a few individuals of *C. bauri* (e.g. AMNH FARB 7234), but not *Megapnosaurus*, the co-ossification between the tibia, fibula, and tarsus is so extensive that co-ossification between the tibia and fibula occurs as well. In these individuals, the rugose bone that covers the posterodistal surfaces

of the tibia and fibula is so extensive that it forms a continuous surface between these two elements. The co-ossification is less obvious in anterior view, analogous to the co-ossification between the tibia and astragalus (character 27). Co-ossification between the tibia and fibula is rare, and I only observed this in five specimens of *C. bauri* (AMNH FARB 7238, AMNH FARB 7234, SMP 858, TMP 1984.63.6, and TMP 1984.63.21). In other individuals the two elements were very closely associated, and may have even been partly co-ossified, but I did not score this character as 'fused' unless the rugose bone was clearly continuous across the suture. Co-ossification between the tibia and fibula has not been reported in other early neotheropods, and I did not observe it in *'Syntarsus' kayentakatae*.

30 Fibula, ridge on medial face of proximal end: (0) absent; (1) present (Fig. 13).

On some fibulae of *Megapnosaurus*, the medial surface of the proximal end is flat and slightly concave laterally with a shallow sulcus, and this sulcus is defined proximally by a sharp border (Fig. 13A). However, other fibulae possess a rounded ridge proximal to this sulcus (which is usually deeper in these individuals) extending from a posteroproximal position on the medial face anterodistally, and the sharp border proximal to this sulcus is absent (Fig. 13B). Rowe and Gauthier (1990) refer to the development of this sulcus as ontogenetic, but for *Megapnosaurus* the ridge was more often variable than is the sulcus it bordered, and the absence or presence of the ridge was more easily diagnosed than the relative depth of the sulcus. The ridge also distally borders a shallow, less well-defined sulcus, and both sulci are deepest near the ridge, and tend to grow shallower away from this ridge. Even individuals without the ridge still preserve thin lineations on the cortical bone of this area, and Rowe & Gauthier (1990) hypothesize that the sulcus is the site of origin of a portion of the pedal flexor musculature.

Nesbitt et al. (2009b) found this ridge on the medial face of the proximal end of the fibula to be a synapomorphy of Neotheropoda (character 314, ACCTRAN optimization), and so it would be expected to be present and ontogenetically variable in *Coelophysis* as well. However, the medial surface of the proximal end of the fibula was covered in all individuals of *C. bauri* for which I attempted to score this character, and so this character was not scored for *C. bauri*. Because this is my only ontogenetic character on the fibula and the fibulae of *M. rhodesiensis* were nearly all isolated specimens, this character was not scored in conjunction with other characters in many specimens of *M. rhodesiensis*. Because of these limitations this character could not be used for OSA in either *C. bauri* or *M. rhodesiensis*, and the small sample size prevents the level of variation in developmental patterns from being confidently determined; however, this character is clearly ontogenetic and does relate to body size because most individuals of *M. rhodesiensis* possessing the mature character state are larger than immature individuals (Fig. 13C). Because this character is clearly ontogenetic, it could prove informative in analyses of other taxa in which preservation does not hinder the scoring of this character.

31 Tarsal III and metatarsal III, co-ossification: (0) absent; (1) present (Fig. 14).

Tarsal III fuses completely to the proximal surface of metatarsal III in some individuals of both *Coelophysis* and *Megapnosaurus* (e.g. MCZ 9433; QG 1029). This results in tarsal III forming a rounded mound extending proximally

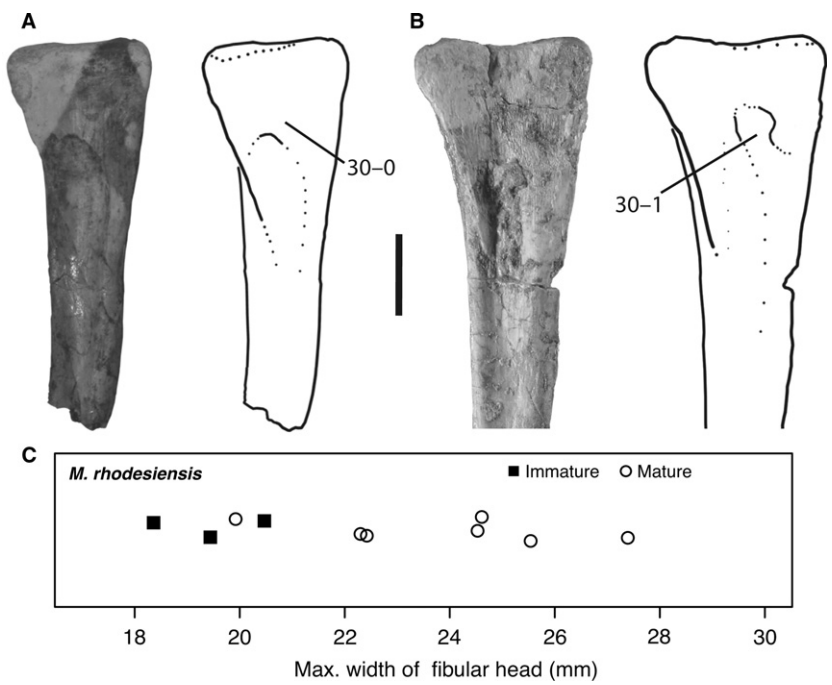

Fig. 13 (A) Photograph (left) and line drawing (right) of left fibula of *Megapnosaurus rhodesiensis* (QG 811) in medial view possessing the immature character state for character 30. (B) Photograph (left) and line drawing (right) of left fibula of *M. rhodesiensis* (QG 813) in medial view possessing the mature character state for character 30. (C) The mature state for the fibular scar (character 30) is mostly present in larger individuals, and the immature state in some of the smallest individuals, but the small fibular sample size and difficulty in scoring articulated specimens make OSA difficult to perform on this character, and to determine how variable this character is with respect to body size. The *y*-axis is dimensionless. Scale bar: 1 cm.

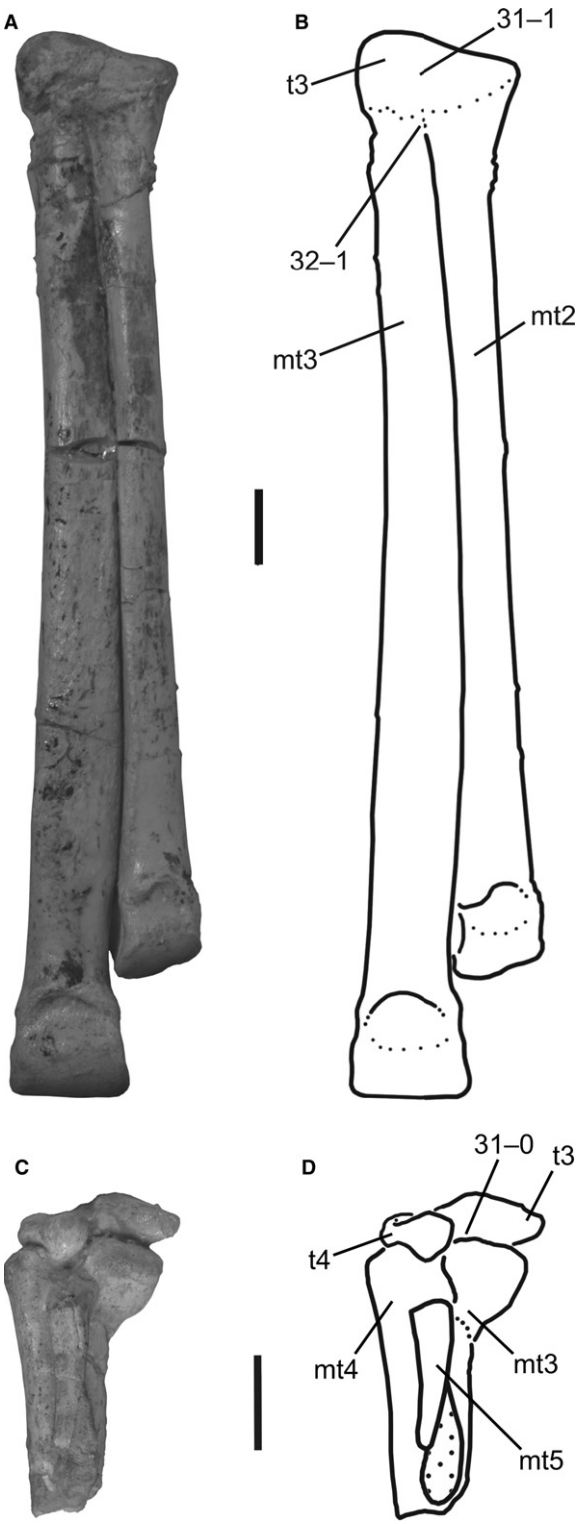

Fig. 14 (A) Photograph and (B) line drawing of right tarsal III and metatarsals II and III of *Megapnosaurus rhodesiensis* (QG 1029) possessing mature character states in anterior view. (C) Photograph and (D) line drawing of the left tarsals III and IV and left metatarsals III–V of *M. rhodesiensis* (QG unnumbered #1) showing immature character states in posterior view. Scale bars: 1 cm. mt2, metatarsal II; mt3, metatarsal III; mt4, metatarsal IV; mt5, metatarsal V; t3, tarsal III; t4, tarsal 4.

from the surface of metatarsal III; the proximal surface of metatarsal III without tarsal III is relatively flat. The co-ossification of these two elements is so complete that it is difficult to determine where one element begins and another ends.

Rowe (1986), Colbert (1989, 1990), and Rowe & Gauthier (1990) all considered tarsals II and III to be present in at least some coelophysoid theropods, and for co-ossification to occur between them as well as their respective metatarsals (although Colbert, 1990, did not consider this to be a function of size or age). However, Tykoski (2005) did not consider any tarsal II to be present in these early neotheropods and therefore did not consider these taxa to possess fused tarsals or tarsal II fused to metatarsal II. Tykoski (2005) also reports that tarsal III slightly covers the proximal end of metatarsal II in *'Syntarsus' kayentakatae*, and that tarsal III–metatarsal III co-ossification is present in the Shake-N-Bake taxon. Nesbitt (2011) found that lacking an ossified tarsal II is a synapomorphy of the clade *Erythrosuchus* + Archosauria, and I follow this in interpreting tarsal II as being unossified in *Coelophysis* and *Megapnosaurus*.

32 Metatarsal II and metatarsal III, co-ossification at proximal ends: (0) absent; (1) present (Fig. 14).

The proximal ends of metatarsals II and III fuse completely in some individuals of both *Coelophysis* and *Megapnosaurus*, and although this co-ossification has been reported to be related to size in *Megapnosaurus* (Raath, 1969, 1977), Colbert (1990) did not consider this co-ossification to be related to size or age in *Coelophysis*. This co-ossification has been interpreted as ontogenetic in early theropods by others (Rowe, 1989; Tykoski, 2005). *'Syntarsus' kayentakatae* (MNA V2623) exhibits this co-ossification, as do other specimens referred to this taxon, although one individual exhibits this co-ossification of the metatarsals on the right pes, but not the left (TMM 43688-1, Tykoski, 2005). The proximal ends of metatarsals II and III are not known from many other early neotheropods, although the shafts of these elements are pressed together tightly in the holotype of *S. halli*, suggesting they may have been fused in this individual (Tykoski, 2005).

Neurocentral suture fusion

Neurocentral sutures fuse during ontogeny, forming the neural arch and centrum into one continuous structure. This has been used with success as a morphological indicator of maturity in extant crocodylians, which possess a posterior-to-anterior sequence of suture closures during ontogeny, with the axis suture closure indicative of the attainment of morphological maturity (Brochu, 1996). This pattern has also been observed in the ontogeny of phytosaurs (Irmis, 2007). However, Irmis (2007) noted that this pattern does not appear to be widespread throughout Archosauria, and that the utility of this pattern (or even the closure of

neurocentral sutures themselves) for determining ontogenetic stage should be evaluated for each clade. Nevertheless, many studies of archosaurian ontogeny have used neurocentral suture fusion to assess the level of maturity attained by an individual with varying degrees of confidence (e.g. Tykoski, 1998; Hutt et al. 2001; Carrano et al. 2005; Makovicky et al. 2005; Fowler et al. 2011; Hofmann & Sander, 2014; Griffin & Nesbitt, 2016a). However, I have observed individuals of *Branta canadensis* (e.g. FMNH 496812) and *Meleagris gallopavo* (e.g. FMNH 461781) that possessed fully closed neurocentral sutures with immature body sizes, skeletal characters (i.e. those of Griffin & Nesbitt, 2016b), and bone textures (i.e. those of Tumarkin-Deratzian et al. 2006). The timing and pattern of neurocentral suture fusion is not consistent across Dinosauria (Irmis, 2007; Hone et al. 2016). Among squamates, the timing of neurocentral suture closure is variable between and within taxa, with some possessing closed sutures as neonates and others only reaching full closure at maximum body size (Maisano, 2002). All this suggests that closure of neurocentral sutures may not necessitate cessation of growth.

I was not able to use neurocentral suture fusion as an ontogenetic character in my ontogenetic analyses, although I did make a note of the state of the sutures in the individuals that I scored for other ontogenetic characters. In all specimens of *C. bauri* I observed the neurocentral sutures were entirely fused in all vertebrae (i.e. suture either obliterated or fused while remaining visible), regardless of the size of the individual or the location of the element(s) in the vertebral column, and so were uninformative with respect to OSA. Vertebrae of *M. rhodesiensis*, in contrast, commonly possess open neurocentral sutures, although many possess closed sutures as well. Unfortunately, the majority of the vertebrae attributable to *M. rhodesiensis* are isolated elements, making the determination of a pattern(s) of neurocentral suture fusion, and how it relates to other ontogenetic characters, impossible. However, all the distalmost caudals I observed possessed closed neurocentral sutures, and one specimen (QG 408) comprised four trunk vertebrae in a series, with the anterior two vertebrae possessing closed neurocentral sutures and the posterior vertebra possessing an open suture. Size does not appear to be strongly related to vertebral suture fusion in *M. rhodesiensis*, although I did not quantitatively evaluate this relationship, and comparing size across different vertebral elements is inexact. Additionally, the large amount of sequence polymorphism in other ontogenetic characters (Griffin & Nesbitt, 2016b; this study) suggests that multiple sequences of neurocentral suture fusion may occur in different individuals of this taxon.

Results

The results of the ontogenetic sequence analyses (OSA) of *Megapnosaurus* and *Coelophysis* are summarized in Table 1. These analyses strongly suggest that sequence polymorphism is present in the ontogenetic trajectories of these taxa (Figs 15–17). Most strikingly, analysis of the full-body dataset of *C. bauri*, consisting of 27 ontogenetic characters, returned 136 ontogenetic sequences (Fig. 15). This sequence polymorphism was not simply the result of variation in growth between elements – analyses of only the femoral dataset (Fig. 16A), the pelvic dataset (Fig. 17D), and the lower leg dataset (Fig. 17A) gave similar results for *Coelophysis*. Additionally, this variation was not caused by variation between classes of ontogenetic characters (i.e. between co-ossification events and bone scar appearance events) because there was a large amount of variation in datasets composed solely of each class of character (Fig. 16C,D). Because almost all specimens of *M. rhodesiensis* were disarticulated, I was unable to construct a full-body dataset like that of *Coelophysis*; however, I obtained similar levels of sequence polymorphism in analyzing femoral characters (Fig. 16B). Because of this disarticulation, I was only able to use six characters to analyze the development of the tibia and tarsus of this taxon, and excluded the two pedal characters used in the tibia-tarsus-pes analysis of *C. bauri*. Surprisingly, this tibiotarsal OSA of *Megapnosaurus* returned only a single ontogenetic sequence of four developmental steps (Fig. 17B), despite the relatively large sample size (Table 1). The ontogenetic sequence analysis of the *C. bauri* pelvic and sacral ontogenetic characters returned 16 ontogenetic sequences reconstructed for the five ontogenetic characters, with a reasonably large amount of sequence polymorphism for such few characters (Fig. 17D; Table 1). However, an analysis of the same characters in *M. rhodesiensis* returned only three distinct ontogenetic sequences (Fig. 17E). Finally, the OSA of the four ontogenetic characters of the humerus of *M. rhodesiensis* yielded only two developmental sequences (Fig. 17C; Table 1). This is unsurprising, given the low number of both characters and specimens analyzed.

Discussion

Differences between *Coelophysis* and *Megapnosaurus*

The most obvious difference between *C. bauri* and *M. rhodesiensis* is the difference in character state changes during ontogeny. Four ontogenetic characters were variable in *M. rhodesiensis* but not in *C. bauri*: the scar on the humerus for the origin of the m. *triceps brachii caput mediale* (character 5–1); the shallow groove on the proximal surface of the femur (character 11–0); the depression on the anterolateral face of the proximal portion of the femur (character 12–0); and the anterolateral edge of the proximal surface of the femur extending anterolaterally (character 13–1). Because these characters are ontogenetically variable, it may be that all observed specimens of *C. bauri* were simply at the incorrect ontogenetic status to possess these

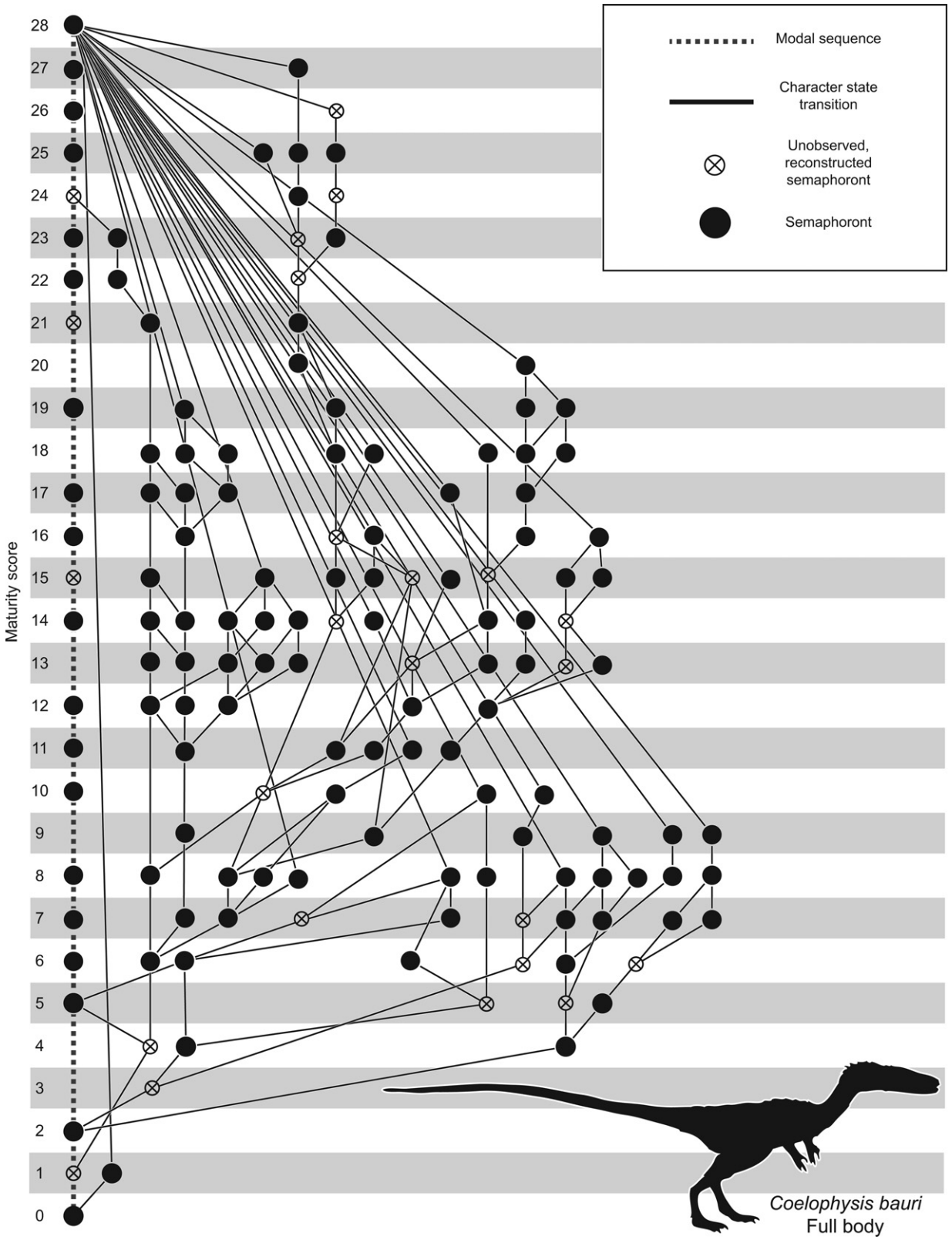

Fig. 15 OSA reticulating diagram showing all 136 equally parsimonious reconstructed developmental sequences for the full-body dataset of 27 ontogenetic characters of *Coelophysis bauri*, modified from Griffin & Nesbitt (2016b). Developmental sequences proceed from the least to most mature semaphoront. Maturity score which represents the number of developmental events undergone by an individual; the x-axis is dimensionless and is only used for visual clarity.

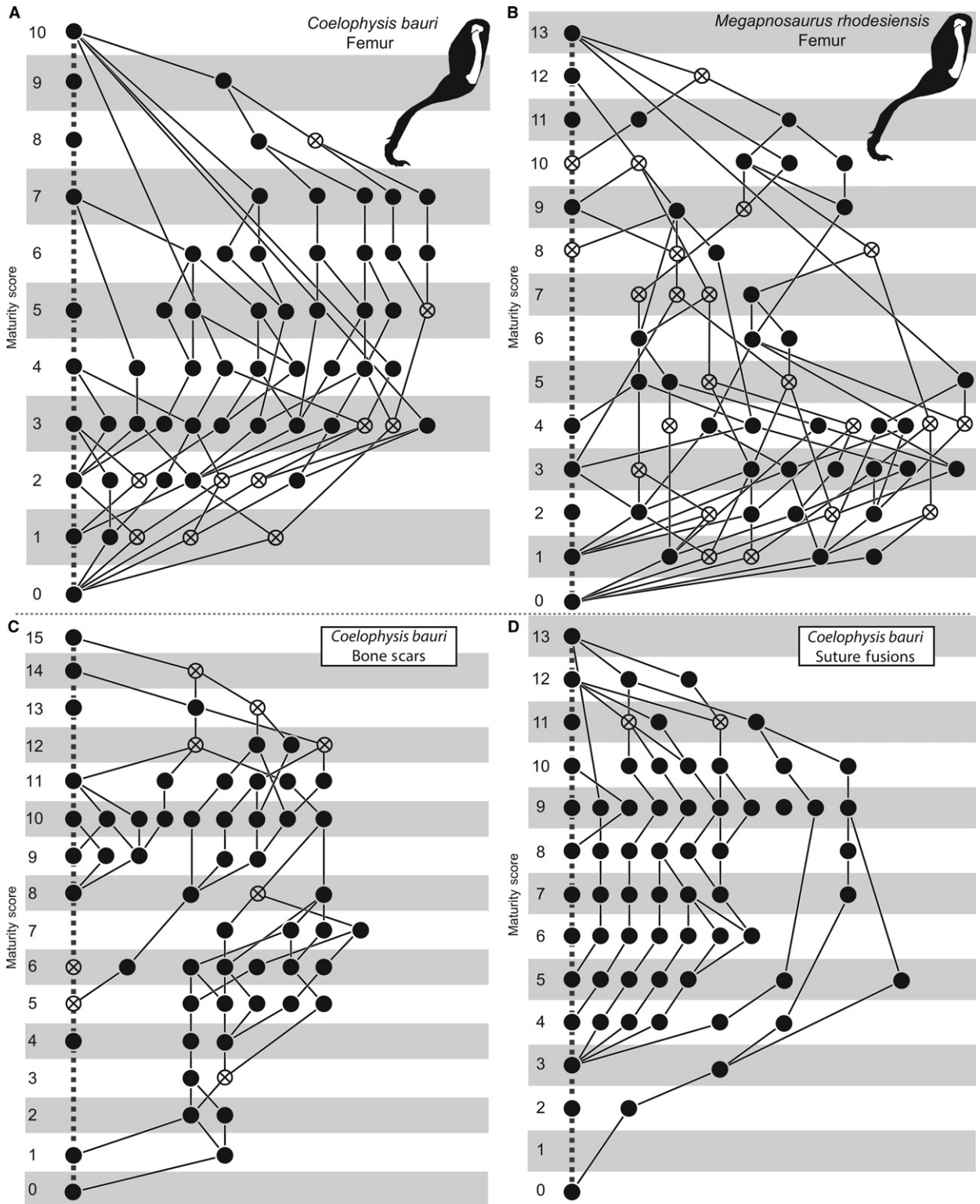

Fig. 16 (A) OSA reticulating diagram showing all 82 equally parsimonious reconstructed developmental sequences for the femoral dataset of 10 ontogenetic characters of *Coelophysis bauri*. (B) OSA reticulating diagram showing all 145 equally parsimonious reconstructed developmental sequences for the femoral dataset of 10 ontogenetic characters of *Megapnosaurus rhodesiensis*. (C) OSA reticulating diagram showing all 74 equally parsimonious reconstructed developmental sequences for the 15 bone scar ontogenetic characters of *C. bauri*. (D) OSA reticulating diagram showing all 27 equally parsimonious reconstructed developmental sequences for the 12 sutural co-ossification ontogenetic characters of *C. bauri*. Both (A) and (B) modified from Griffin & Nesbitt (2016b). Key follows Fig. 15.

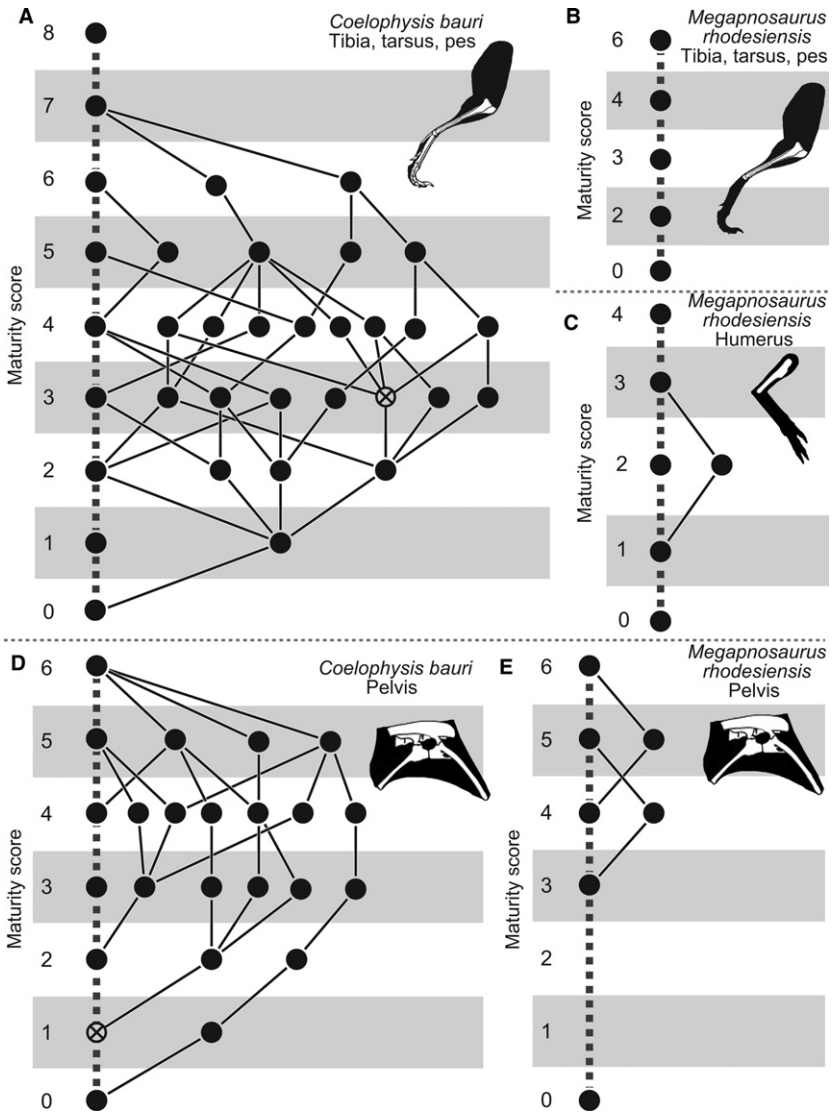

Fig. 17 (A) OSA reticulating diagram showing all 35 equally parsimonious reconstructed developmental sequences for the tibial, tarsal, and pedal dataset of eight ontogenetic characters of *Coelophysis bauri*. (B) OSA reticulating diagram showing the single parsimonious reconstructed developmental sequence for the tibial dataset of 6 ontogenetic characters of *Megapnosaurus rhodesiensis*. (C) OSA reticulating diagram showing both equally parsimonious reconstructed developmental sequences for the humeral dataset of four ontogenetic characters of *M. rhodesiensis*. (D) OSA reticulating diagram showing all 16 equally parsimonious reconstructed developmental sequences for the pelvic dataset of five ontogenetic characters of *C. bauri*. (E) OSA reticulating diagram showing all three equally parsimonious reconstructed developmental sequences for the pelvic dataset of five ontogenetic characters of *M. rhodesiensis*. Key follows Fig 15.

character states. If this is the case, this difference in characters still represents a difference between taxa because, unlike the other ontogenetic characters, the ontogenetic sequence of these characters is so different that they can be misinterpreted as absent in one taxon. If all the characters apparently absent from *C. bauri* were all the immature or mature states, this would suggest that the observed individuals of *C. bauri* are too immature/mature, respectively, to possess these states, and would therefore leave open the possibility that these characters were present in *C. bauri* but unobserved because of a sample that does not include the individuals possessing the requisite stages of maturity to observe these states. However, this is not the case: two of the anomalous character states are the mature state, whereas for the other two characters it is the immature state that is absent in the *C. bauri* sample. This suggests that these are clear morphological differences between the taxa, and that *C. bauri* would lack these anatomical features regardless of the level of maturity attained. *M. rhodesiensis* is larger on average than *C. bauri* and sizes are not multimodally distributed in either taxon (Fig. 18).

These data also suggest that *C. bauri* and *M. rhodesiensis* grew differently, with different ontogenetic sequences reconstructed for the same elements and characters for these taxa, although the majority of the features that changed during ontogeny are the same, and they reached roughly similar sizes at maturity. Most strikingly, *M. rhodesiensis*, unlike *C. bauri*, appears to lack sequence polymorphism in the ontogenetic characters of the tibia and tarsus, although this lack of variation may simply be a result of using only four characters in the analysis of *Megapnosaurus*. Additionally, the developmental sequence of certain characters may be invariable, even when the sequence of these characters with respect to other characters is variable. To properly assess the amount of sequence polymorphism in a taxon, it is preferable to include as many

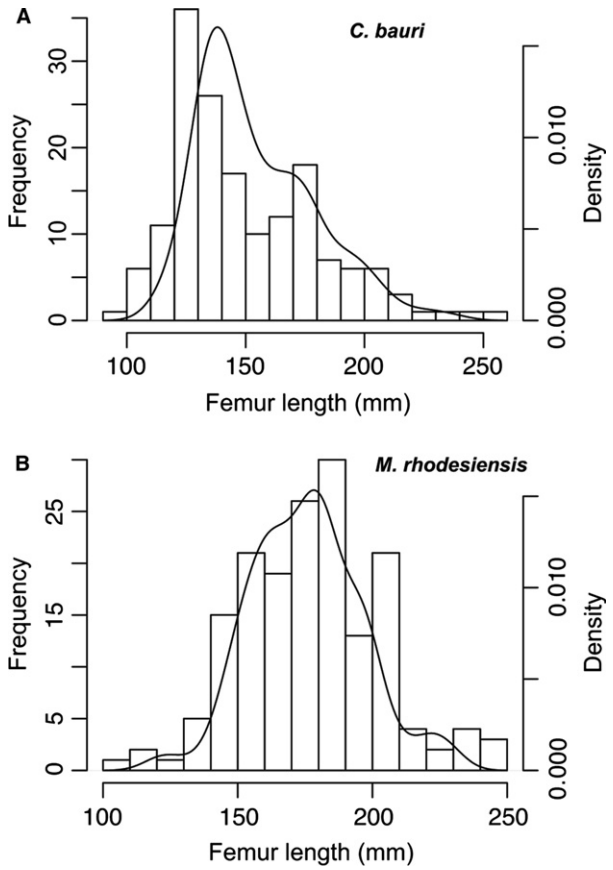

Fig. 18 (A) Size distribution of individuals of *Coelophysis bauri* by femoral length, shown as frequency of bins (left y-axis) and kernel density (right y-axis). (B) Size distribution of individuals of *Megapnosaurus rhodesiensis* by femoral length, shown as frequency of bins (left y-axis) and kernel density (right y-axis).

ontogenetic characters across as many elements and anatomical regions as possible.

Ontogenetic variation in *Coelophysis* and *Megapnosaurus*

Both *C. bauri* and *M. rhodesiensis* possess a large amount of variation in the sequence of developmental events undergone during postnatal ontogeny, as well as in the body sizes at which these events occur (Griffin & Nesbitt, 2016b; Figs 15–17). Sequence polymorphism was reconstructed for the ontogenetic characters of all elements analyzed, with the exception of four ontogenetic characters analyzed in the tibia and tarsus of *M. rhodesiensis* (characters 26–29). Although sample size is important for detecting sequence polymorphism (de Jong et al. 2009; Griffin & Nesbitt, 2016a), the large number of individuals used in the analysis of these four characters in *M. rhodesiensis* would preclude this lack of variation as an artefact of low sample size, although this low variation may simply be the result of only analyzing four characters. Therefore, *M. rhodesiensis* appears to lack sequence polymorphism in this portion of the skeleton, although the characters of other elements analyzed, especially the femur, possess sequence polymorphism. Additionally, sequence polymorphism is greater in some elements than in others in both taxa (Table 1), although in some cases this may be an expression of differing sample sizes in *M. rhodesiensis*. Furthermore, bone scars (formed from the attachment of muscles, tendons, and ligaments) possessed a higher level of variation in development than did element co-ossifications in *C. bauri* (Fig. 16C,D; Table 1), although both had large amounts of variation in developmental sequences. Therefore, the characters and elements chosen for analysis can play an important role in the amount of sequence polymorphism interpreted to be possessed by the population in question. Additionally, a large number of ontogenetic characters as well as a large sample size of individuals enables a higher level of confidence in interpreting of sequence polymorphism as being present or absent in a population. The large sample size of both ontogenetic characters and individuals utilized in this study allow the presence of sequence polymorphism to be confidently hypothesized for these taxa.

OSA reconstructs all equally parsimonious developmental pathways and is therefore an excellent method of quantifying the amount of sequence polymorphism in a population for any set of ontogenetic characters (Colbert & Rowe, 2008). However, just because a developmental sequence is reconstructed does not mean that any single individual necessarily underwent this individual sequence during life, and in fact the actual number of developmental sequences in a population could be lower than predicted by OSA. However, OSA cannot distinguish between 'real' developmental sequences and those that are equally parsimonious and simply reconstructed from the data. This difficulty does not exist in a sample with a low amount of sequence polymorphism because the modal sequence represents nearly all individuals in a population and is therefore almost certainly a 'real' sequence undergone by those individuals in life (although a small or skewed sample may underreport variation, e.g. the tibia/tarsus dataset of *Megapnosaurus*). However, with increasing amounts of sequence polymorphism, this certainty lessens for any one sequence, including the modal sequence. This difficulty explains the differences in modal sequences between characters for any single element and the sequence of those characters in the modal sequence of the full-body OSA of characters of *C. bauri* characters (Fig. 19). Because there is so much sequence polymorphism in this taxon, the modal sequences for each analysis only make up a relatively small portion of the total weight of all sequences (Table 1), so relatively small differences in the number of individuals preserved/included may change which sequence is recovered as the modal sequence. Therefore, although OSA is an excellent way to quantify the amount of sequence polymorphism in a

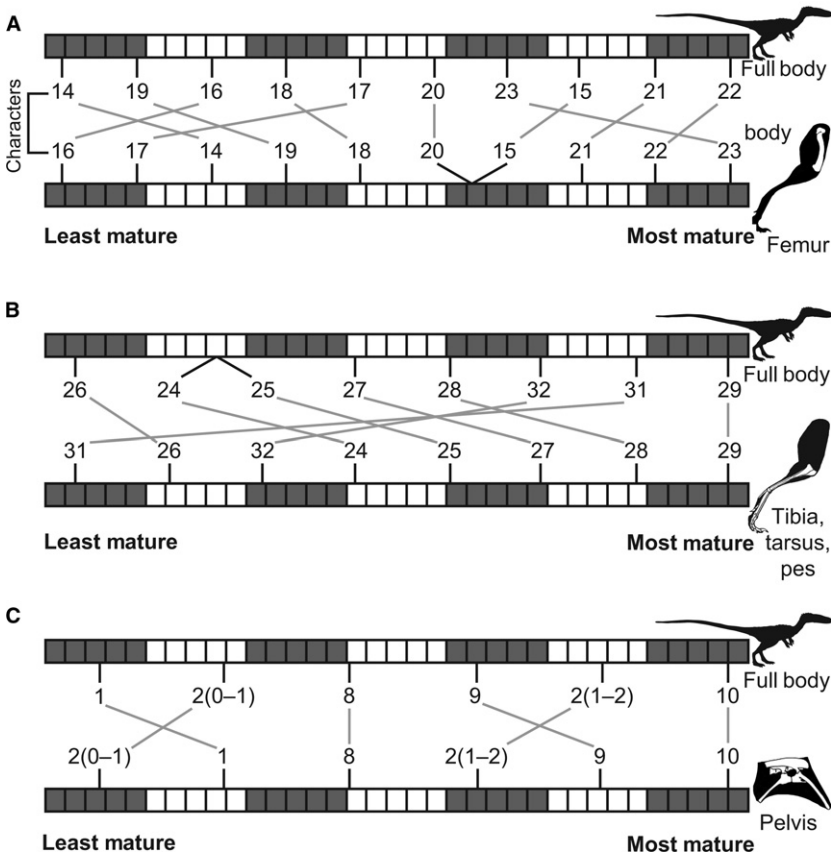

Fig. 19 Comparisons between the modal developmental sequences of the full body dataset and femoral, lower hindlimb (tibia, tarsus, pes), and pelvic datasets of *Coelophysis bauri*. (A) Modal sequence of femoral characters in the full-body OSA (top) and the femoral OSA (bottom). (B) Modal sequence of tibial, tarsal, and pedal characters in the full-body OSA (top) and the tibial, tarsal, and pedal OSA (bottom). (C) Modal sequence of pelvic characters in the full-body OSA (top) and the pelvic OSA (bottom).

population, for a population with a high level of sequence polymorphism the confidence that any one sequence was actually undergone by an individual in the population is lower than that of a population with very low levels of variation. However, at least some reconstructed sequences must have been utilized by individuals in the population given the assumptions of OSA (see Materials and Methods).

Body size commonly is used as a proxy for ontogenetic status and morphological maturity (e.g. Colbert, 1990; Chinnery & Weishampel, 1998; Benton et al. 2000; Hunt, 2001; Currie, 2003; Bybee et al. 2006; Heckert et al. 2006; Buckley et al. 2010; Carpenter, 2010; Piechowski et al. 2014; Griffin & Nesbitt, 2016a). However, ontogenetic status, body size, and morphological maturity as determined by ontogenetic characters may all be somewhat disjunctive, with similarly sized individuals possessing differing levels of morphological maturity in early dinosaurs (Griffin & Nesbitt, 2016b), and perhaps even in all non-avian dinosaurs (Hone et al. 2016). For example, TMP 1984.063.0001 #1, a larger-than-average individual of *C. bauri* (measured femoral length = 158.1 mm), possesses a suite of entirely immature character states (Fig. 20), whereas MNA V3318, a smaller individual (measured femoral length = 124.7 mm), possesses many mature character states (Fig. 21), and the smallest known individual of *M. rhodesiensis* (estimated femoral length = 111.95 mm) possesses a large, robust trochanteric shelf (character 14–1; 15–1). Although the YPM *Coelophysis* material was not included in the presented analyses, a relatively large individual (YPM 41197; tibia length = 192.5 mm; estimated femur length = 177.9 mm) possesses a partially co-ossified astragalus and calcaneum with a clear, open line of suture, and no other tibial-tarsal co-ossification (Supporting Information Fig. S11). The co-ossification of the astragalus and calcaneum is one of the first characters to move from an immature to mature state (character 26; Fig. 22A), so an immature state in a relatively large individual – one that possesses a fully co-ossified scapula and coracoid, and tarsal III and metatarsal III – is another striking instance of the variation in both form and size in this population. A similarly poor correlation between ontogenetically variable characters and body size has been reported for many early dinosaurs and dinosauriforms (e.g. Benton et al. 2000; Britt et al. 2000; Carrano et al. 2002; Sander & Klein, 2005; Tykoski, 2005; Klein & Sander, 2007; Griffin & Nesbitt, 2016a,b), although preliminary analyses of similar (or even homologous) ontogenetic characters are far better correlated with size in extant birds (Griffin & Nesbitt, 2016b). Future, extensive histological investigation of *C. bauri* and *M. rhodesiensis* may determine whether size is a good indicator of ontogenetic age (with differences in morphological maturity reflecting variation in absolute timing of ontogenetic characters), but this is beyond the scope of this study.

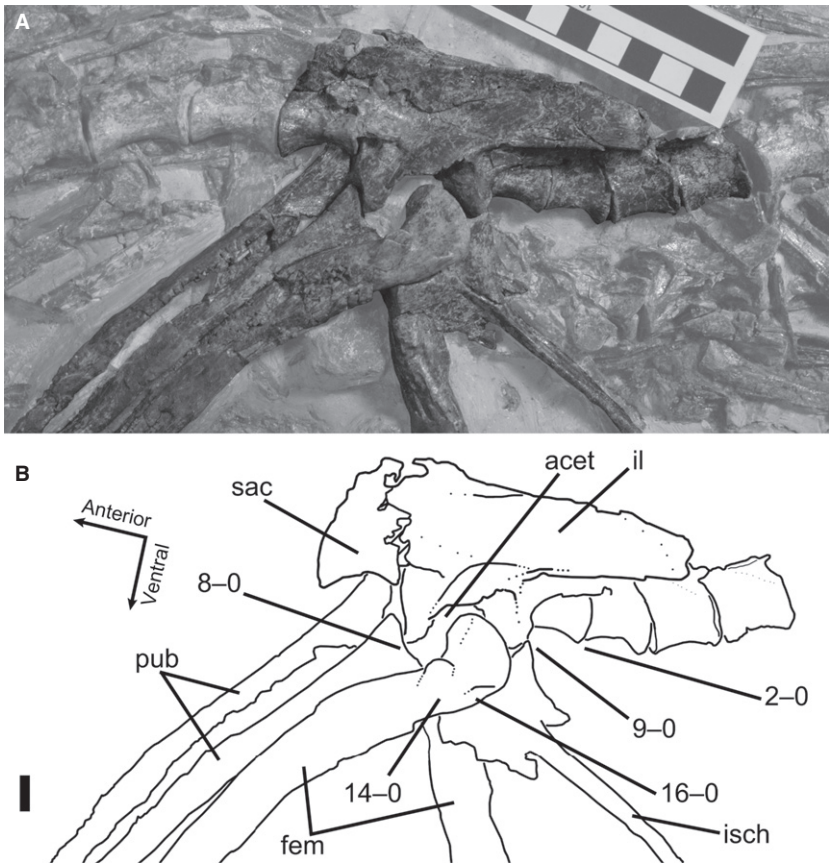

Fig. 20 (A) Photograph and (B) line drawing of a relatively large individual of *Coelophysis bauri* (TMP 1984.063.0001, #1) that possesses entirely immature character states in lateral view. Non-target skeletal elements and matrix have been lightened in PHOTOSHOP to highlight relevant skeletal elements. Scale bar: 1 cm. acet, acetabulum; fem, femur; il, ilium; isch, ischium; pub, pubis; sac, sacrum.

Although a preliminary report suggests that this relationship holds (Chinsamy, 1990), more recent work suggests that histology among *Megapnosaurus* individuals (Werning, 2013) may be somewhat variable with respect to histological maturity and body size. Many larger individuals with more lines of arrested growth (LAGs) and indicators of slowed growth also possess more indicators of morphological maturity (e.g. QG 731, 753). However, the smallest individual, with only one LAG (QG 45; Chinsamy, 1990; Werning, 2013), possesses a trochanteric shelf, so this relationship between histological and morphological maturity does have exceptions. Among several other early dinosauriforms (Nesbitt et al. 2013; Griffin & Nesbitt, 2016a) histology may not be informative as to precise ontogenetic status or individual ontogenetic age.

Neurocentral suture fusion of all vertebrae apparently occurs very early in ontogeny among the majority of individuals of *C. bauri*, because all vertebrae that could be confidently identified as belonging to this taxon possessed coossified elements, regardless of body size or ontogenetic character states. Similarly, the neurocentral suture of all cervical vertebrae of the type specimen of *'Syntarsus' kayentakatae* are fused (Tykoski, 1998). In contrast, most of the vertebrae of *M. rhodesiensis* possess open neurocentral sutures, with the exception of the distalmost caudal vertebrae. Because one partial series of trunk vertebrae possessed fused neurocentral sutures in the anterior vertebrae, the sequence of vertebral fusion may proceed anteriorly from the caudal vertebrae and posteriorly from the dorsals in this taxon, with the posterior dorsals or sacrals the last the fuse their neurocentral sutures. However, the large amount of sequence polymorphism in other elements in this taxon may suggest that more than one sequence of neurocentral suture fusion exists within the population. Although the complete fusion of neurocentral sutures indicates the attainment of skeletal maturity and cessation of growth in extant crocodylians (Brochu, 1996; Irmis, 2007), the absence of open neurocentral sutures in any individual of *C. bauri*, no matter the size or suite of ontogenetic character states, suggests that this is not a universal means of determining whether skeletal growth has ceased in an individual.

Implications for development in early dinosaurs and their close relatives

How the earliest dinosaurs changed morphologically during ontogeny is poorly understood. Therefore, assessing the relative ontogenetic status attained by an individual before death based on gross morphological features has been difficult for these taxa. Although osteohistology is useful for determining skeletal maturity (e.g. Horner et al. 1999, 2000; Erickson & Tumanova, 2000; Erickson et al. 2004), it is a

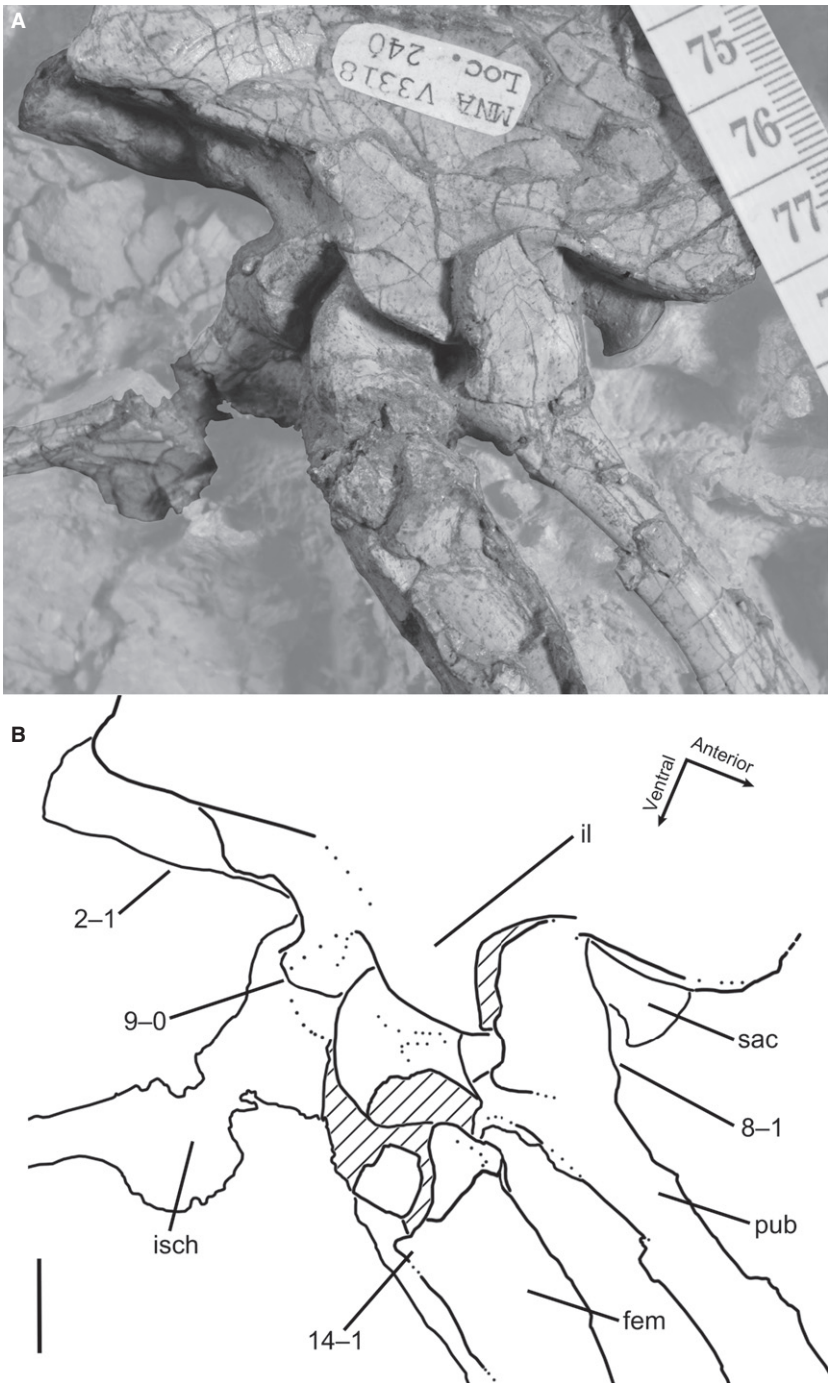

Fig. 21 (A) Photograph and (B) line drawing of a smaller individual of *Coelophysis bauri* (MNA V3318) which possesses many mature character states in left dorsolateral view. Non-target skeletal elements and matrix have been lightened in PHOTOSHOP to highlight relevant skeletal elements. Scale bar: 1 cm. fem, femur; il, ilium; isch, ischium; pub, pubis; sac, sacrum.

destructive process and the utility of the information gained may be highly variable depending on the element sampled and osteohistological features present (e.g. annual growth lines). Even with the large amount of sequence polymorphism that is present in my datasets, some ontogenetic characters reach mature character states at consistently earlier developmental stages than others in *C. bauri* (Fig. 22A). If this average relative order is conserved across early theropods or dinosaurs, then these characters may be important indicators of the level of maturity attained by an individual, even if known from only partial or fragmentary remains. For example, co-ossification of the tibia and fibula (character 29), the ilium and ischium (character 9), and the pubis and ischium (character 10) are indicative of morphological maturity because these character states appear later in morphological maturity. Conversely, lack of co-ossification of the scapula and coracoid (character 1), astragalus and calcaneum (character 26), metatarsals II and III (character 32), and a ridge-like dorsolateral trochanter (character 16) would strongly indicate that an individual is immature,

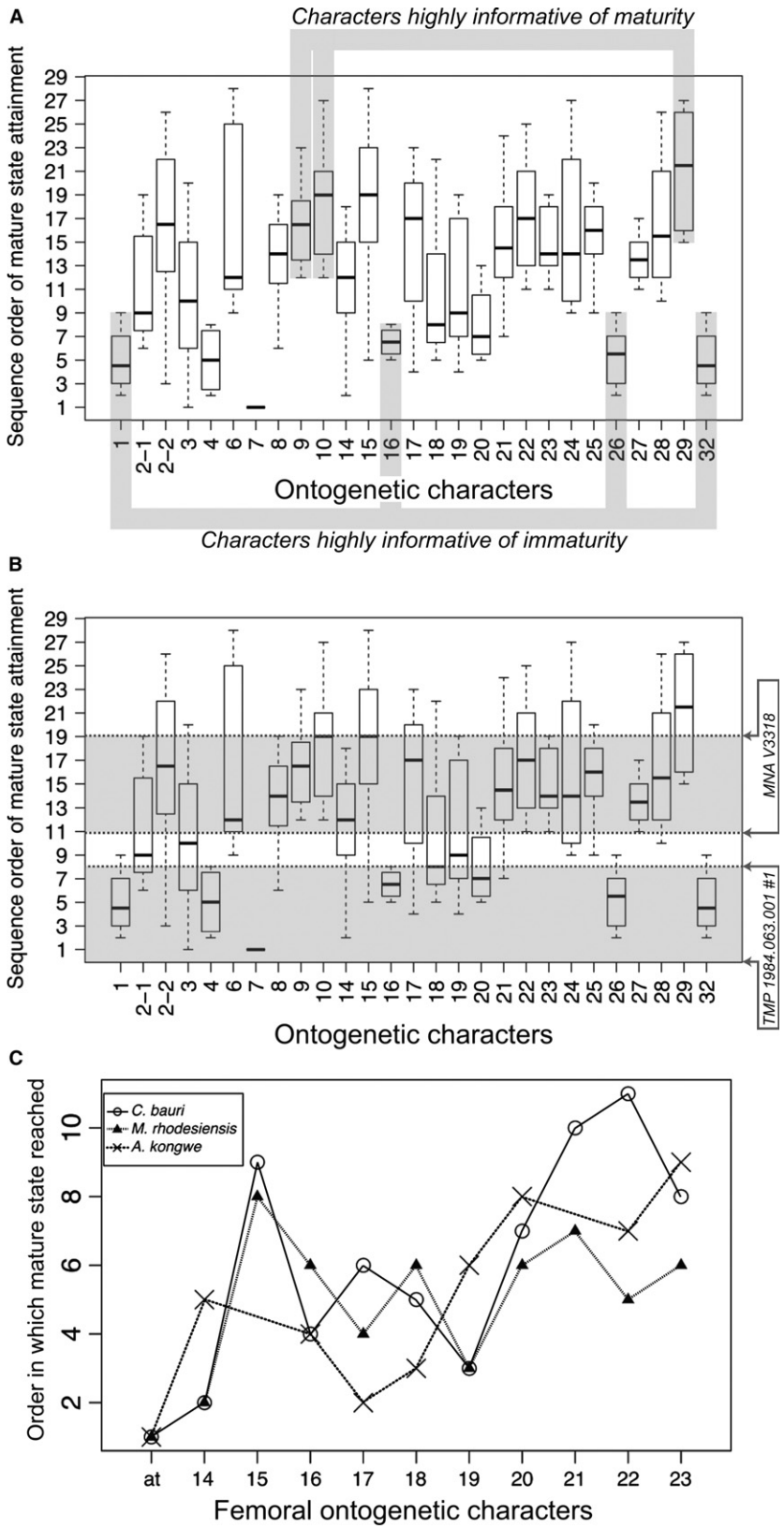

Fig. 22 (A) The range of orders in OSA sequences that each ontogenetic character attains mature state in the full-body OSA of *Coelophysis bauri*, with characters that are particularly informative for assessing morphological maturity highlighted. Character 2 is an ordered character with three states. (B) The suite of character states an individual possesses can be informative with respect to its state of maturity. A larger individual (TMP 1984.063.0001, #1) may be less mature than a smaller individual (MNA V3318) based on character states. Arrows indicate upper and lower bounds of maturity ranges, based on character states. (C) Modal sequence orders of 11 homologous femoral characters from the femoral OSAs of the theropods *Coelophysis bauri* and *Megapnosaurus rhodesiensis*, and of the silesaurid *Asilisaurus kongwe*. Anterior trochanter is abbreviated at, and because it is present in all known individuals of *C. bauri* and *M. rhodesiensis*, it is considered to have appeared first in ontogeny in these taxa. All other character numbers follow those of this study. *A. kongwe* OSA data taken from Griffin & Nesbitt (2016a).

because these characters are some of the first to attain mature states in ontogeny (Fig. 22A). Additionally, an individual complete enough to possess a suite of character states may be compared with the OSAs of *C. bauri* and *M. rhodesiensis* to assist in the determination of relative maturity of that individual, provided that the

developmental characters utilized are phylogenetically bracketed for the taxon being assessed (see Fig. 22B to see this method utilized in two individuals of *C. bauri*).

Properly understanding the morphological changes undergone during ontogeny is also important for reconstructing evolutionary relationships. The fact that phylogenetic characters can be ontogenetically variable has been touched on in many studies – a skeletally immature specimen of a given taxon may be recovered in a very different, often more basal phylogenetic position relative to a mature specimen of the same taxon (Tykoski, 1998, 2005; Carr, 1999; Carr & Williamson, 2004; Fredrickson & Tumarkin-Deratzian, 2014). Therefore, understanding what phylogenetic characters are variable in ontogeny, and how the scoring of these characters influences the phylogenetic placement of taxa that may only be known from immature individuals, is important for properly reconstructing evolution (Butler & Zhao, 2009; Evans et al. 2011; Fowler et al. 2011; Tsuihiji et al. 2011; Campione et al. 2013; Tsai & Fordyce, 2014). This problem has been especially noted in early dinosaurs and their relatives, which possess many phylogenetically important characters that are variable during development (Tykoski, 2005; Griffin & Nesbitt, 2016a,b; Barta et al. 2018; Wang et al. 2017). Characters such as the presence/absence of the trochanteric shelf, which is highly variable throughout ontogeny and among individuals (Griffin & Nesbitt, 2016a,b), may have to be excluded from or highly altered in analyses to provide phylogenetically informative patterns. Variation within a population is the foundation of natural selection, and how the morphology of a population varies must be characterized and integrated into the construction of characters.

This intraspecific variation in anatomical characters may affect basic taxonomy in the earliest dinosaurs in their close relatives, clades for which few species are known from more than one to four fragmentary individuals (Langer, 2004; Langer & Benton, 2006), which can in turn affect our understanding of the diversity and paleobiogeography of these taxa. Because of this variation, individuals of a poorly sampled taxon might be spuriously considered to represent multiple taxa because of seemingly unique character combinations caused by developmental variation and sequence polymorphism. For example, the early neotheropod *Lophostropheus airelensis* was hypothesized to be congeneric with *L. liliensterni*, in part based on the perceived shared characters of unfused sacral vertebrae and fused sacral ribs (Cuny & Galton, 1993). However, these ontogenetically variable characters are widespread among early neotheropods (Ezcurra & Cuny, 2007) and given the high variation present in the ontogeny of *C. bauri* and *M. rhodesiensis*, it is not surprising that this individual would have fused sacral ribs and unfused sacral vertebrae. Therefore, knowledge of what anatomical features are variable within a species and their level of variation can aid in supporting or rejecting taxonomic assignment of specimens.

Although there is variation in the order at which mature character states are reached, comparing modal sequences across taxa may help determine what ontogenetically variable phylogenetic characters are more useful, and which should be used with caution. In comparing the order of appearance of homologous femoral ontogenetic characters between three early dinosauriforms with excellent growth series, *C. bauri*, *M. rhodesiensis,* and the silesaurid *A. kongwe* (Griffin & Nesbitt, 2016a), some characters consistently appear earlier in ontogeny than others, and the order of appearance during ontogeny is fairly conserved across early dinosauriformes (Fig. 22C). For example, the appearance of the anterior trochanter is probably one of the first, if not the first, ontogenetically variable phylogenetic character to appear during ontogeny, and will probably not influence the results of a phylogenetic analysis even if many immature specimens are included in the analysis. Conversely, a character such as the insertion scar of the *m. caudifemoralis brevis* (character 22) may present more problems for phylogenetic analysis, because this character appears in a range of ontogenetic orders in these taxa, all later in ontogeny. In this case, a taxon only known from skeletally or morphologically immature individuals is more likely to appear to lack this character (and others like it) because of ontogenetic status. Additionally, because many phylogenetic characters for early dinosaurs and other archosaurs are based on the morphology of muscle scars (e.g. dorsolateral trochanter, anterior trochanter, trochanteric shelf, fourth trochanter; Nesbitt, 2011), which can change throughout postnatal ontogeny, these characters should be used with caution in cladistic analyses of archosaurs and their closest relatives. However, simply deleting these characters from a cladistic analysis is unwarranted, because this will remove potentially useful information. Scoring a character state known to be ontogenetically variable as missing data for an individual that may be skeletally immature is a feasible way to circumvent this problem (Tykoski, 2005), as may coding such a character as multistate. Multiple high-profile conflicting hypotheses regarding the relationships of early dinosaurs and their kin have recently been proposed (e.g. Nesbitt et al. 2009b, 2010; Cabreira et al. 2016; Baron et al. 2017) and some of this uncertainty may derive from the widespread amount of ontogenetic and intraspecific variation present among these groups (Griffin & Nesbitt, 2016b). Determining which characters are variable, the amount by which they vary, and how to treat these characters properly in phylogenetic analyses may prove crucial to reaching consensus on the relationships of early dinosaurs and their relatives.

Acknowledgements

I thank the curators and collections staff at AMNH, CM, CMNH, FMNH, GR, MCZ, MNA, NMMNH, QG, SMP, TMP, UCM, and UMNH. This study was enriched by discussions with R. Irmis, P. Makovicky,

N. Smith, M. McClain, S. Werning, K. Padian, K. Stein, A. Marsh, A. Pritchard, and Z. Morris, D. Barta, and the VT Paleobiology Research Group. I thank my committee members S. Nesbitt, M. Stocker, M. Colbert, and L. Freeman, as well as A. Marsh, P. Makovicky, and an anonymous referee, for their helpful reviews of the manuscript. This study was supported by the Jurassic Foundation, a Geological Society of America Graduate Student Research Grant, the Charles E. and Frances P. Sears Research Scholarship, and a National Science Foundation Graduate Research Fellowship.

I have no conflicts of interest to declare.

References

Andrews CW (1921) On some remains of a theropodous dinosaur from Scotland: limb bone of a ceratosaur theropod from Skye. *Scott J Geol* **31**, 177–182.

Bailleul AM, Scannella JB, Horner JR, et al. (2016) Fusion patterns in the skulls of modern archosaurs reveal that sutures are ambiguous maturity indicators for the Dinosauria. *PLoS One* **11**, e0147687.

Ballman P (1969) Les oiseaux Miocènes de La Grive-Saint-Alban (Isère). *Gèobios* **2**, 157–204.

Baron MG, Norman DB, Barrett PM (2017) A new hypothesis of dinosaur relationships and early dinosaur evolution. *Nature* **543**, 501–506.

Barta DE, Nesbitt SJ, Norell MA (2018) The evolution of the manus of early theropod dinosaurs is characterized by high inter- and intraspecific variation. *J Anat* **232**, 80–104.

Bennett SC (1993) The ontogeny of *Pteranodon* and other pterosaurs. *Paleobiology* **19**, 92–106.

Bennett SC (1996) Year-classes of pterosaurs from the Solnhofen Limestone of Germany: taxonomic and systematic implications. *J Vertebr Paleontol* **16**, 432–444.

Benton MJ, Juul L, Storrs GW, et al. (2000) Anatomy and systematics of the prosauropod dinosaur *Thecodontosaurus antiquus* from the Upper Triassic of southwest England. *J Vertebr Paleontol* **20**, 77–108.

Bristowe A, Raath MA (2004) A juvenile coelophysoid skull from the Early Jurassic of Zimbabwe, and the synonymy of *Coelophysis* and *Syntarsus*. *Palaeontologia Africana* **40**, 31–41.

Britt BB, Chure DJ, Holtz TRJ, et al. (2000) A reanalysis of the phylogenetic affinities of *Ceratosaurus* (Theropoda, Dinosauria) based on new specimens from Utah, Colorado, and Wyoming. *J Vertebr Paleontol* **20**, 32A.

Brochu CA (1992) Ontogeny of the postcranium in crocodylomorph archosaurs. Department of Geological Sciences. pp. 340, Austin: University of Texas at Austin.

Brochu CA (1996) Closure of neurocentral sutures during crocodilian ontogeny: implications for maturity assessment in fossil archosaurs. *J Vertebr Paleontol* **16**, 49–62.

Brochu CA (2003) Osteology of *Tyrannosaurus rex*: insights from a nearly complete skeleton and high-resolution computed tomographic analysis of the skull. *J Vertebr Paleontol*, **22** (Suppl. to 4), 1–138.

Brusatte SL, Nesbitt SJ, Irmis RB, et al. (2010) The origin and early radiation of dinosaurs. *Earth Sci Rev* **101**, 68–100.

Buckley LG, Larson DW, Reichel M, et al. (2010) Quantifying tooth variation within a single population of *Albertosaurus sarcophagus* (Theropoda: Tyrannosauridae) and implications for identifying isolated teeth of tyrannosaurids. *Can J Earth Sci* **47**, 1227–1251.

Burch SH (2014) Complete forelimb myology of the basal theropod dinosaur *Tawa hallae* based on a novel robust muscle reconstruction method. *J Anat* **225**, 271–297.

Burch SH (2017) Myology of the forelimb of *Majungasaurus crenatissimus* (Theropoda, Abelisauridae) and the morphological consequences of extreme limb reduction. *J Anat* **231**, 515–531.

Butler RJ (2010) The anatomy of the basal ornithischian dinosaur *Eocursor parvus* from the lower Elliot Formation (Late Triassic) of South Africa. *Zool J Linn Soc* **160**, 648–684.

Butler RJ, Zhao Q (2009) The small-bodied ornithischian dinosaurs *Micropachycephalosaurus hongtuyanensis* and *Wannanosaurus yansiensis* from the Late Cretaceous of China. *Cretac Res* **30**, 63–77.

Bybee PJ, Lee AH, Lamm E-T (2006) Sizing the Jurassic theropod dinosaur *Allosaurus*: assessing growth strategy and evolution of ontogenetic scaling of limbs. *J Morphol* **267**, 347–359.

Cabreira SF, Kellner AWA, Dias-de-Silva S, et al. (2016) A unique Late Triassic dinosauromorph assemblage reveals dinosaur ancestral anatomy and diet. *Curr Biol* **26**, 1–6.

Camp CL (1930) A study of the phytosaurs with description of new material from western North America. *Memoirs of the University of California* **10**, 1–175.

Campione N, Brink KS, Freedman EA, et al. (2013) '*Glishades ericksoni*', an indeterminate juvenile hadrosaurid from the Two Medicine Formation of Montana: implications for hadrosauroid diversity in the latest Cretaceous (Campanian-Maastrichtian) of western North America. *Palaeodiv Palaeoenviron* **93**, 65–75.

Carpenter K (1997) A giant coelophysoid (Ceratosauria) theropod from the Upper Triassic of New Mexico. *Neues Jb Geol Paläontol* **205**, 189–208.

Carpenter K (2010) Variation in a population of Theropoda (Dinosauria): *Allosaurus* from the Cleveland-Lloyd Quarry (Upper Jurassic), Utah, USA. *Paleontol Res* **14**, 250–259.

Carr TD (1999) Craniofacial ontogeny in Tyrannosauridae (Dinosauria, Coelosauria). *J Vertebr Paleontol* **19**, 497–520.

Carr TD, Williamson TE (2004) Diversity of late Maastrichtian Tyrannosauridae (Dinosauria: Theropoda) from western North America. *Zool J Linn Soc* **142**, 149–523.

Carrano MT, Hutchinson JR (2002) Pelvic and hindlimb musculature of *Tyrannosaurus rex* (Dinosauria: Theropoda). *J Morphol* **253**, 207–228.

Carrano MT, Sampson SD (1999) Evidence for a paraphyletic 'Ceratosauria' and its implications for theropod dinosaur evolution. *J Vertebr Paleontol* **19**, 36A.

Carrano MT, Sampson SD, Forster CA (2002) The osteology of *Masiakasaurus knopfleri*, a small abelisauroid (Dinosauria: Theropoda) from the Late Cretaceous of Madagascar. *J Vertebr Paleontol* **22**, 510–534.

Carrano MT, Hutchinson JR, Sampson SD (2005) New information of *Segisaurus halli*, a small theropod dinosaur from the Early Jurassic of Arizona. *J Vertebr Paleontol* **25**, 835–849.

Chinnery BJ, Weishampel DB (1998) *Montanoceratops cerorhynchus* (Dinosauria: Ceratopsia) and relationships among basal neoceratopsians. *J Vertebr Paleontol* **18**, 569–585.

Chinsamy A (1990) Physiological implications of the bone histology of *Syntarsus rhodesiensis* (Saurischia: Theropoda). *Palaeontol Africana* **27**, 77–82.

Chinsamy A (1993) Bone histology and growth trajectory of the prosauropod dinosaur *Massospondylus carinatus* Owen. *Modern Geol* **18**, 319–329.

Codron D, Carbone C, Müller DWH, et al. (2012) Ontogenetic niche shifts in dinosaurs influenced size, diversity and extinction in terrestrial vertebrates. *Biol Let* **8**, 620–623.

Colbert EH (1989) The Triassic dinosaur *Coelophysis*. *Museum Northern Arizona Bull* **57**, 1–160.

Colbert EH (1990) Variation in *Coelophysis bauri*. In *Dinosaur Systematics: Perspectives and Approaches* (eds Carpenter K, Currie PJ), pp. 81–90. Cambridge: Cambridge University Press, 356 pp.

Colbert MW, Rowe T (2008) Ontogenetic sequence analysis: using parsimony to characterize developmental sequences and sequence polymorphism. *J Exp Zool Part B Mol Develop Evol* **310B**, 398–416.

Coria RA, Chiappe LM, Dingus L (2002) A new close relative of *Carnotaurus sastrei* Bonaparte 1985 (Theropoda: Abelisauridae) from the Late Cretaceous of Patagonia. *J Vertebr Paleontol* **22**, 460–465.

Cracraft J (1971) The functional morphology of the hind limb of the Domestic Pigeon, *Columba livia*. *Bull Am Mus Nat Hist* **144**, 171–268.

Crush PJ (1984) A Late Upper Triassic sphenosuchid crocodilian from Wales. *Palaeontology* **27**, 131–157.

Cuny G, Galton PM (1993) Revision of the Airel theropod dinosaur from the Triassic-Jurassic boundary. *Neues Jb Geol Paläontol Abh* **187**, 261–288.

Currie PJ (2003) Cranial anatomy of tyrannosaurid dinosaurs from the Late Cretaceous of Alberta, Canada. *Acta Palaeontol Pol* **48**, 191–226.

Delfino M, Sánchez-Villagra MR (2010) A survey of the rock record of reptilian ontogeny. *Semin Cell Dev Biol* **21**, 432–440.

Dilkes DW (2000) Appendicular myology of the hadrosaurian dinosaur *Maiasaura peeblesorum* from the Late Cretaceous (Campanian) of Montana. *Transact R Soc Edinburgh Earth Sci* **90**, 87–125.

Dutuit J-M (1979) Un pseudosuchien du Trias continental marocain. *Ann Paléontol (Vertébrés)* **65**, 55–68.

Dzik J (2003) A beaked herbivorous archosaur with dinosaur affinities from the early Late Triassic of Poland. *J Vertebr Paleontol* **23**, 556–574.

Erickson GM, Tumanova TA (2000) Growth curve of *Psittacosaurus mongoliensis* Osborn (Ceratopsia: Psittacosauridae) inferred from long bone histology. *Zool J Linn Soc* **130**, 551–566.

Erickson GM, Mackovicky PJ, Currie PJ, et al. (2004) Gigantism and comparative life-history parameters of tyrannosaurid dinosaurs. *Nature* **430**, 772–775.

Evans DC, Brown CM, Ryan MJ, et al. (2011) Cranial ornamentation and ontogenetic status of *Homalocephale calathocercos* (Ornithischia: Pachycephalosauria) from the Nemegt Formation, Mongolia. *J Vertebr Paleontol* **31**, 84–92.

Ezcurra MD (2006) A review of the systematic position of the dinosauriform archosaur *Eucoelophysis baldwini* Sullivan & Lucas, 1999 from the Upper Triassic of New Mexico, USA. *Geodiversitas* **28**, 649–684.

Ezcurra MD (2016) The phylogenetic relationships of basal archosauromorphs, with an emphasis on the systematics of proterosuchian archosauriforms. *PeerJ* **4**, e1778.

Ezcurra MD, Brusatte SL (2011) Taxonomic and phylogenetic reassessment of the early neotheropod dinosaur *Camposaurus arizonensis* from the Late Triassic of North America. *Palaeontology* **54**, 763–772.

Ezcurra MD, Cuny G (2007) The coelophysoid *Lophostropheus airelensis*, gen. nov.: a review of the systematics of *'Liliensternus' airelensis* from the Triassic-Jurassic outcrops of Normandy (France). *J Vertebr Paleontol* **27**, 73–86.

Ferigolo J, Langer MC (2006) A Late Triassic dinosauriform from south Brazil and the origin of the ornithischian predentary bone. *Hist Biol* **19**, 1–11.

Forster CA (1999) Gondwanan dinosaur evolution and biogeographic analysis. *J Afr Earth Sc* **28**, 169–185.

Fowler DW, Woodward HN, Freedman EA, et al. (2011) Reanalysis of '*Raptorex kriegsteini*': a juvenile tyrannosaurid dinosaur from Mongolia. *PLoS One* **6**, e21376.

Fredrickson JA, Tumarkin-Deratzian AR (2014) Craniofacial ontogeny in *Centrosaurus apertus*. *PeerJ* **2**, e252.

Galton PM (1982) Juveniles of the stegosaurian dinosaur *Kentrosaurus* from the Upper Jurassic of Tanzania, East Africa. *J Vertebr Paleontol* **2**, 47–62.

Galton PM (1990) Basal sauropodomorpha – prosauropoda. In: *The Dinosauria*. 1st edn (eds Weishampel DB, Dodson P, Osmólska H), pp. 320–344. Berkeley: University of California Press.

Gauthier JA (1984) A cladistic analysis of the higher systematic categories of the Diapsida, pp. 564. Berkeley: University of California, PhD dissertation.

Gay R (2005) Sexual dimorphism in the Early Jurassic theropod dinosaur *Dilophosaurus* and a comparison with other related forms. In: *The Carnivorous Dinosaurs* (ed. Carpenter K), pp. 277–283. Indianapolis: Indiana University Press.

Genin D (1992) Hind limb proportions and ontogenetic changes in the theropod dinosaur, *Coelophysis bauri*, pp. 107. DeKalb: Northern Illinois University, MS thesis.

Gilmore CW (1920) Osteology of the carnivorous Dinosauria in the United States National Museum, with special reference to the genera *Antrodemus* (*Allosaurus*) and *Ceratosaurus*. *Bull U S Natl Museum* **110**, 1–154.

Griffin CT, Nesbitt SJ (2016a) The histology and femoral ontogeny of the Middle Triassic (?late Anisian) dinosauriform *Asilisaurus kongwe* and implications for the growth of early dinosaurs. *J Vertebr Paleontol* **36**, e1111224.

Griffin CT, Nesbitt SJ (2016b) Anomalously high variation in growth is ancestral for dinosaurs but lost in birds. *Proc Natl Acad Sci U S A* **113**, 14757–14762.

Heckert AB, Lucas SG, Rinehart LF, et al. (2006) Revision of the archosauromorph reptile *Trilophosaurus*, with a description of the first skull of *Trilophosaurus jacobsi*, from the Upper Triassic Chinle Group, West Texas, USA. *Palaeontology* **49**, 621–640.

Hennig WE (1966) *Phylogenetic Systematics*, p. 280. Urbana: University of Illinois Press.

Hofmann R, Sander PM (2014) The first juvenile specimens of *Plateosaurus engelhardti* from Frick, Switzerland: isolated neural arches and their implications for developmental plasticity in a basal sauropodomorph. *PeerJ* **2**, e458.

Holtz TRJ (1994) The phylogenetic position of the Tyrannosauridae: implications for theropod systematics. *J Paleontol* **68**, 1100–1117.

Holtz TRJ, Osmólska H (2004) Saurischia. In: *The Dinosauria*. 2nd edn (eds Weishampel DB, Dodson P, Osmólska H), pp. 21–24. Berkeley: University of California Press.

Hone DWE, Farke AA, Wedel WJ (2016) Ontogeny and the fossil record: what, if anything, is an adult dinosaur? *Biol Let* **12**, 20150947.

Horner JR, Goodwin MB (2009) Extreme cranial ontogeny in the Upper Cretaceous dinosaur *Pachycephalosaurus*. *PLoS One* **4**, e7626.

Horner JA, Padian K (2004) Age and growth dynamics of *Tyrannosaurus rex*. *Proc R Soc B Biol Sci* **271**, 1875–1880.

Horner JA, Ricqlès A, Padian K (1999) Variation in dinosaur skeletochronology indicators: implications for age assessment and physiology. *Paleobiology* **25**, 295–304.

Horner JA, Ricqlès A, Padian K (2000) Long bone histology of the hadrosaurid dinosaur *Maiasaura peeblesorum*: growth dynamics and physiology based on an ontogenetic series of skeletal elements. *J Vertebr Paleontol* **20**, 109–123.

Horner JA, Padian K, Ricqlès A (2001) Comparative osteohistology of some embryonic and perinatal archosaurs: developmental and behavioral implications for dinosaurs. *Paleobiology* **27**, 39–58.

Hunt AP (2001) The vertebrate fauna, biostratigraphy, and biochronology of the type Revueltian land-vertebrate faunachron, Bull Canyon Formation (Upper Triassic), east-central New Mexico. New Mexico Geological Society 52nd Field Conference Guidebook, 123–151.

Hutchinson JR (2001) The evolution of femoral osteology and soft tissues on the line to extant birds (Neornithes). *Zool J Linn Soc* **131**, 169–197.

Hutchinson JR (2002) The evolution of hindlimb tendons and muscles on the line to crown-group birds. *Comp Biochem Physiol A Mol Integr Physiol* **133**, 1051–1086.

Hutchinson JR, Anderson FC, Blemker SS, et al. (2005) Analysis of hindlimb muscle moment arms in *Tyrannosaurus rex* using a three-dimensional musculoskeletal computer model: implications for stance, gait, and speed. *Paleobiology* **31**, 676–701.

Hutt S, Naish D, Martill DM, et al. (2001) A preliminary account of a new tyrannosauroid theropod from the Wessex Formation (Early Cretaceous) of southern England. *Cretac Res* **22**, 227–242.

Irmis RB (2007) Axial skeleton ontogeny in the parasuchia (Archosauria: Pseudosuchia) and its implications for ontogenetic determination in archosaurs. *Zool J Linn Soc* **131**, 169–197.

Irmis RB, Nesbitt SJ, Padian K, et al. (2007) A Late Triassic dinosauromorph assemblage from New Mexico and the rise of dinosaurs. *Science* **317**, 358–361.

Ivie MA, Slipinski SA, Wegrzynowicz P (2001) Generic homonyms in the Colydiinae (Coleoptera: Zopheridae). *Insecta Mundi* **15**, 63–64.

Jasinoski SC, Russell AP, Currie PJ (2006) An integrative phylogenetic and extrapolatory approach to the reconstruction of dromaeosaur (Theropoda: Eumaniraptora) shoulder musculature. *Zool J Linn Soc* **146**, 301–344.

Johnson R (1977) Size independent criteria for estimating relative age and the relationships among growth parameters in a group of fossil reptiles (Reptilia: Ichthyosauria). *Can J Earth Sci* **14**, 1916–1924.

de Jong IML, Colbert MW, Wittle F, et al. (2009) Polymorphism in developmental timing: intraspecific heterochrony in a Lake Victoria cichlid. *Evolut Develop* **7**, 367–394.

Klein N, Sander PM (2007) Bone histology and growth of the prosauropod *Plateosaurus engelhardti* MEYER, 1837 from the Norian bonebeds of Trossingen (Germany) and Frick (Switzerland). *Special Papers in Paleontology*, 169–206.

Knoll FK, Padian K, Ricqlès A (2010) Ontogenetic change and adult body size of the early ornithischian dinosaur *Lesothosaurus diagnosticus*: implications for basal ornithischian taxonomy. *Gondwana Res* **17**, 171–179.

Langer MC (2003) The pelvic and hind limb anatomy of the stem-sauropodomorph *Saturnalia tupiniquim* (Late Triassic, Brazil). *PaleoBios* **23**, 1–30.

Langer MC (2004) Basal Saurischia. In: *The Dinosauria*. 2nd edn (eds Weishampel DB, Dodson P, Osmólska H), pp. 25–46. Berkeley: University of California Press.

Langer MC, Benton MJ (2006) Early dinosaurs: a phylogenetic study. *J Syst Paleontol* **4**, 309–358.

Langer MC, Ferigolo J (2013) The Late Triassic dinosauromorph *Sacisaurus agudoensis* (Caturrita Formation; Rio Grande do Sul, Brazil): anatomy and affinities. In: *Anatomy, Phylogeny, and Palaeobiology of Early Archosaurs and Their Kin* (eds Nesbitt SJ, Desojo JB, Irmis RB), pp. 353–392. London: Geological Society.

Langer MC, Franca MAG, Gabriel S (2007) The pectoral girdle and forelimb anatomy of the stem-sauropodomorph *Saturnalia tupiniquim* (Upper Triassic, Brazil). *Spec Papers Paleontol*, 77.

Larson P (2013) The case for *Nanotyrannus*. In: *Tyrannosaurid Paleobiology* (eds Parrish JM, Molnar RE, Currie PJ, Koppelhus EB), pp. 15–54. Bloomington: Indiana University Press.

Lee MSY (1996) The homologies and early evolution of the shoulder girdle in turtles. *Proc R Soc B Biol Sci* **263**, 111–117.

Lloyd GT (2016) Estimating morphological diversity and tempo with discrete character-taxon matrices: implementation, challenges, progress, and future directions. *Biol J Linn Soc* **118**, 131–151.

Maddison DR, Maddison WP (2002) *MacClade 4: Analysis of Phylogeny and Character Evolution. Version 1.04*. Sunderland: Simauer Associates.

Madsen JH, Welles SP (2000) *Ceratosaurus* (Dinosauria, Theropoda): a revised osteology. *Utah Geol Surv Miscell Publ* **00–2**, 1–80.

Madsen JHJ (1976) *Allosaurus fragilis*: a revised osteology. *Utah Geol Surv Bullet* **109**, 1–163.

Maechler M (2015) diptest: Hartigan's Dip Test Statistic for Unimodality – Corrected. *R package version 0.75-7*.

Maisano JA (2002) Terminal fusions of skeletal elements as indicators of maturity in squamates. *J Vertebr Paleontol* **22**, 268–275.

Makovicky PJ, Apesteguía S, Agnolín FL (2005) The earliest dromaeosaurid theropod from South America. *Nature* **437**, 1007–1011.

Marsh OC (1884) Principal characters of American Jurassic dinosaurs, part VIII: The order Theropoda. *Am J Sci* **27**, 329–340.

Marsh OC (1892) Restorations of claosaurus and ceratosaurus. *Am J Sci* **44**, 343–349.

Martill DM, Frey E, Sues H-D, et al. (2000) Skeletal remains of a small theropod dinosaur with associated soft structures from the Lower Cretaceous Santana Formation of northeastern Brazil. *Can J Earth Sci* **37**, 891–900.

Martill DM, Vidovic SU, Howells C, et al. (2016) The oldest Jurassic dinosaur: a basal neotheropod from the Hettangian of Great Britain. *PLoS One* **11**, e0145713.

Martínez RN, Giménez O, Rodríguez J, et al. (1986) *Xenotarsosaurus bonapartei* nov. gen. et sp. (Carnosauria, Abelisauridae), un nuevo Theropoda de la Formación Bajo Barreal, Chubut, Argentina. *Simposio de Evolucion de los vertebrados Mesozoicos: IV Congreso Argentino de paleontologia y bioestratigrafia* **2**, 23–31.

Martínez RN, Apaldetti C, Correa GA, et al. (2015) A Norian lagerpetid dinosauromorph from the Quebrada del Barro Formation, northwestern Argentina. *Ameghiniana* **53**, 1–13.

Meers MB (2003) Crocodylian forelimb musculature and its relevance to Archosauria. *Anat Rec* **274A**, 891–916.

Morris Z (2013) Skeletal ontogeny of *Monodelphis domestica* (Mammalia: Didelphidae): quantifying variation, variability, and technique bias in ossification sequence reconstruction, pp. 204. Austin: University of Texas at Austin, MS thesis.

Nesbitt SJ (2011) The early evolution of archosaurs: relationships and the origin of major clades. *Bull Am Mus Nat Hist* **352**, 1–292.

Nesbitt SJ, Ezcurra MD (2015) The early fossil record of dinosaurs in North America: a new neotheropod from the base of the Upper Triassic Dockum Group of Texas. *Acta Palaeontol Pol* **60**, 513–526.

Nesbitt SJ, Irmis RB, Parker WG (2007) A critical re-evaluation of the Late Triassic dinosaur taxa of North America. *J Syst Paleontol* **5**, 209–243.

Nesbitt SJ, Irmis RB, Parker WG, et al. (2009a) Hindlimb osteology and distribution of basal dinosauromorphs from the Late Triassic of North America. *J Vertebr Paleontol* **29**, 498–516.

Nesbitt SJ, Smith ND, Irmis RB, et al. (2009b) A complete skeleton of a Late Triassic saurischian and the early evolution of dinosaurs. *Science* **326**, 1530–1533.

Nesbitt SJ, Sidor CA, Irmis RB, et al. (2010) Ecologically distinct dinosaurian sister group shows early diversification of Ornithodira. *Nature* **464**, 95–98.

Nesbitt SJ, Barrett PM, Werning S, et al. (2013) The oldest dinosaur? A Middle Triassic dinosauriform from Tanzania. *Biol Let* **9**, 20120949.

Novas FE (1993) New information on the systematics and postcranial skeleton of *Herrerasaurus ischigualastensis* (Theropoda: Herrerasauridae) from the Ischigualasto Formation (Upper Triassic) of Argentina. *J Vertebr Paleontol* **13**, 400–423.

Novas FE (1996) Dinosaur monophyly. *J Vertebr Paleontol* **16**, 723–741.

Novas FE, Salgado L, Suárez M, et al. (2015) An enigmatic plant-eating theropod from the Late Jurassic period of Chile. *Nature* **522**, 331–334.

Padian K, Ricqlès A, Horner JA (2001) Dinosaurian growth rates and bird origins. *Nature* **412**, 405–408.

Padian K, Horner JA, Ricqlès A (2004) Growth in small dinosaurs and pterosaurs: the evolution of archosaurian growth strategies. *J Vertebr Paleontol* **24**, 555–571.

Piechowski R, Tałanda M, Dzik J (2014) Skeletal variation and ontogeny of the Late Triassic Dinosauriform *S. opolensis*. *J Vertebr Paleontol* **34**, 1383–1393.

Raath MA (1969) A new coelurosaurian dinosaur from the Forest Sandstone of Rhodesia. *Arnoldia Rhodesia* **4**, 1–25.

Raath MA (1977) The anatomy of the Triassic theropod *Syntarsus rhodesiensis* (Sauischia: Podokesauridae) and a consideration of its biology, pp. 233. Grahamstown, South Africa: Rhodes University, PhD Dissertation.

Raath MA (1990) Morphological variation in small theropods and its meaning in systematics: evidence from *Syntarsus rhodesiensis*. In: *Dinosaur Systematics: Perspectives and Approaches* (eds Carpenter K, Currie PJ), pp. 91–105. Cambridge: Cambridge University Press.

Rauhut OWM (2003) The interrelationships and evolution of basal dinosaurs. *Special Papers Paleontol* **69**, 1–214.

Ricqlés A (1968) Recherches paléohistologiques sur les os longs des Tétrapodes. I. Origine du tissu osseux plexiforme des Dinosauriens Sauropodes. *Ann Paléontol (Vertébrés)* **54**, 133–145.

Rinehart LF, Lucas SG, Heckert AB, et al. (2009) The paleobiology of *Coelophysis bauri* (Cope) from the Upper Triassic (Apachean) Whitaker Quarry, New Mexico, with detailed analysis of a single quarry block. *New Mexico Mus Nat Hist Sci Bull* **45**, 1–260.

Romer A (1956) *Osteology of the Reptiles*. Chicago: University of Chicago Press.

Rowe T (1986) Homology and evolution of the deep dorsal thigh musculature in birds and other Reptilia. *J Morphol* **189**, 327–346.

Rowe T (1989) A new species of the theropod dinosaur *Syntarsus* from the Early Jurassic Kayenta Formation of Arizona. *J Vertebr Paleontol* **9**, 125–136.

Rowe T, Gauthier J (1990) Ceratosauria. In: *The Dinosauria*. 1st edn (eds Weishampel DB, Dodson P, Osmólska H), pp. 151–168. Berkeley: University of California Press.

Sander PM, Klein N (2005) Developmental plasticity in the life history of a prosauropod dinosaur. *Science* **16**, 1800–1802.

Sander PM, Klein N, Buffetaut E, et al. (2004) Adaptive radiation in sauropod dinosaurs: bone histology indicates rapid evolution of giant body size through acceleration. *Org Divers Evol* **4**, 165–173.

Scanella JB, Horner JR (2010) *Torosaurus* Marsh, 1891, is *Triceratops* Marsh, 1889 (Ceratopsidae: Chasmosaurinae): synonymy through ontogeny. *J Vertebr Paleontol* **30**, 1157–1168.

Schachner ER, Manning PL, Dodson P (2011) Pelvic and hindlimb myology of the basal archosaur *Poposaurus gracilis* (Archosauria: Poposauroidea). *J Morphol* **272**, 1464–1491.

Schwartz HL, Gillette DD (1994) Geology and taphonomy of the *Coelophysis* quarry, Upper Triassic Chinle Formation, Ghost Ranch, New Mexico. *J Paleontol* **68**, 1118–1130.

Sereno PC (1991) Lesothosaurus, 'fabrosaurids', and the early evolution of Ornithischia. *J Vertebr Paleontol* **11**, 168–197.

Sereno PC (1994) The pectoral girdle and forelimb of the basal theropod *Herrerasaurus ischigualastensis*. *J Vertebr Paleontol* **13**, 425–450.

Sereno PC, Arcucci AB (1994) Dinosaurian precursors from the Middle Triassic of Argentina: *Marasuchus lilloensis*, gen. nov. *J Vertebr Paleontol* **14**, 53–73.

Sereno PC, Wilkinson M, Conrad JL (2004) New dinosaurs link southern landmasses in the Mid-Cretaceous. *Proc R Soc B Biol Sci* **271**, 1325–1330.

Sereno PC, McAllister S, Brusatte SL (2005) TaxonSearch: a relational database for suprageneric taxa and phylogenetic definitions. *PhyloInformatics* **8**, 1–21.

Sereno PC, Martínez RN, Alcobar OA (2013) Osteology of *Eoraptor lunensis* (Dinosauria, Sauropodomorpha). *J Vertebr Paleontol* **32**, 83–179.

Smith ND, Makovicky PJ, Hammer WR, et al. (2007) Osteology of *Cryolophosaurus ellioti* (Dinosauria: Theropoda) from the Early Jurassic of Antarctica and implications for early theropod evolution. *Zool J Linn Soc* **151**, 377–421.

Sues H-D, Nesbitt SJ, Berman DS, et al. (2011) A late-surviving basal theropod dinosaur from the latest Triassic of North America. *Proc Royal Soc B: Biol Sci* **278**, 3459–3464.

Swofford DL (2003) *PAUP*. Phylogenetic Analysis Using Parsimony (*and Other Methods). Version 4.)*. Sunderland: Sinauer Associates.

Tsai C-H, Fordyce RE (2014) Disparate heterochronic processes in baleen whale evolution. *Evol Biol* **41**, 299–307.

Tsai HP, Holliday CM (2014) Articular soft tissue anatomy of the archosaur hip joint: structural homology and functional implications. *J Morphol* **276**, 601–630.

Tsuihiji T, Watabe M, Togtbaater K, et al. (2011) Cranial osteology of a juvenile specimen of *Tarbosaurus bataar* (Theropoda, Tyrannosauridae) from the Nemegt Formation (Upper Cretaceous) of Bugin Tsav, Mongolia. *J Vertebr Paleontol* **31**, 1–21.

Tumarkin-Deratzian AR, Vann DR, Dodson P (2006) Bone surface texture as an ontogenetic indicator in long bones of the Canada goose *Branta canadensis* (Anseriformes: Anatidae). *Zool J Linn Soc* **148**, 133–168.

Tumarkin-Deratzian AR, Vann DR, Dodson P (2007) Growth and textural ageing in long bones of the American alligator *Alligator mississippiensis* (Crocodylia: Alligatoridae). *Zool J Linn Soc* **150**, 1–39.

Tykoski RS (1998) The osteology of *Syntarsus kayentakatae* and its implications for ceratosaurid phylogeny, pp. 217. Austin: University of Texas Austin, MS thesis.

Tykoski RS (2005) Anatomy, ontogeny, and phylogeny of coelopysoid dinosaurs, pp. 553. Austin: The University of Texas at Austin, PhD dissertation.

Tykoski RS, Rowe T (2004) Ceratosauria. In: *The Dinosauria*. 2nd edn (eds Weishampel DB, Dodson P, Osmólska H), pp. 47–70. Berkeley: University of California Berkeley Press.

Walker AD (1970) A revision of the Jurassic reptile *Hallopus victor* (Marsh), with remarks on the classification of crocodiles. *Philos Trans R Soc B* **257**, 323–372.

Wang S, Stiegler J, Amiot R, et al. (2017) Extreme ontogenetic changes in a ceratosaurian theropod. *Curr Biol* **27**, 144–148.

Weishampel DB, Chapman RE (1990) Morphometric study of Plateosaurus from Trossingen (Baden-Württemberg, Federal Republic of Germany). In: *Dinosaur Systematics: Approaches and Perspectives* (edsCarpenter K, Currie PJ), pp. 43–51. Cambridge: Cambridge University Press.

Welles SP (1984) *Dilophosaurus wetherilli* (Dinosauria, Theropoda) osteology and comparisons. *Palaeont Abt A* **185**, 85–180.

Werning S (2013) *Evolution of Bone Histological Characters in Amniotes, and the Implications for the Evolution of Growth and Metabolism.)*, pp. 445. Berkeley: University of California.

Wilkinson M (1995) Coping with abundant missing entries in phylogenetic inference using parsimony. *Syst Biol* **44**, 501–514.

Wilson JA, Sereno PC, Srivastava S, et al. (2003) A new abelisaurid (Dinosauria, Theropoda) from the Lameta Formation (Cretaceous, Maastrichtian) of India. *Contributions from the Museum of Paleontology, University of Michigan* **31**, 1–42.

You H-L, Azuma Y, Wang T, et al. (2014) The first well-preserved coelophysoid theropod dinosaur from Asia. *Zootaxa* **3873**, 233–249.

Supporting Information

Additional Supporting Information may be found in the online version of this article:

Methods S1. Flowchart showing a simple example of ontogenetic sequence analysis methodology. Refer to Materials and Methods in the main text for precise instructions on conducting OSA.

Methods S2. Transforming trees returned by PAUP* into partial OSA reticulating diagrams.

Fig. S1. Detailed ontogenetic sequence analysis reticulating diagram for the full postcrania dataset of 27 ontogenetic characters of *Coelophysis bauri*.

Fig. S2. Detailed ontogenetic sequence analysis reticulating diagram for the femoral dataset of 10 ontogenetic characters of *Coelophysis bauri*.

Fig. S3. Detailed ontogenetic sequence analysis reticulating diagram for the femoral dataset of 13 ontogenetic characters of *Megapnosaurus rhodesiensis*.

Fig. S4. Detailed ontogenetic sequence analysis reticulating diagram for the tibial, tarsal, and pedal dataset of eight ontogenetic characters of *Coelophysis bauri*.

Fig. S5. Detailed ontogenetic sequence analysis reticulating diagram for the tibial and tarsal dataset of six ontogenetic characters of *Megapnosaurus rhodesiensis*.

Fig. S6. Detailed ontogenetic sequence analysis reticulating diagram for the humeral dataset of four ontogenetic characters of *Megapnosaurus rhodesiensis*.

Fig. S7. Detailed ontogenetic sequence analysis reticulating diagram for the sacral and pelvic dataset of six ontogenetic characters of *Coelophysis bauri*.

Fig. S8. Detailed ontogenetic sequence analysis reticulating diagram for the sacral and pelvic dataset of six ontogenetic characters of *Megapnosaurus rhodesiensis*.

Fig. S9. Detailed ontogenetic sequence analysis reticulating diagram for the suture fusion dataset of 12 ontogenetic characters of *Coelophysis bauri*.

Fig. S10. Detailed ontogenetic sequence analysis reticulating diagram for the bone scar dataset of 15 ontogenetic characters of *Coelophysis bauri*.

Fig. S11. The left tarsus and pes of a fairly large individual of *Coelophysis bauri* (YPM 41197).

Data S1. Specimen scores for 27 ontogenetic characters of *Coelophysis bauri*.

Data S2. Specimen scores for 32 ontogenetic characters of *Megapnosaurus rhodesiensis*.

Data S3. NEXUS file of *Coelophysis bauri* specimens used for the full-body, 27-character ontogenetic sequence analysis. See attached NEXUS file.

Data S4. NEXUS file of *Coelophysis bauri* specimens used for the femoral character ontogenetic sequence analysis. See attached NEXUS file.

Data S5. NEXUS file of *Megapnosaurus rhodesiensis* specimens used for the femoral character ontogenetic sequence analysis. See attached NEXUS file.

Data S6. NEXUS file of *Coelophysis bauri* specimens used for the tibial, tarsal, and pedal character ontogenetic sequence analysis. See attached NEXUS file.

Data S7. NEXUS file of *Megapnosaurus rhodesiensis* specimens used for the tibial and tarsal character ontogenetic sequence analysis. See attached NEXUS file.

Data S8. NEXUS file of *Megapnosaurus rhodesiensis* specimens used for the humeral character ontogenetic sequence analysis. See attached NEXUS file.

Data S9. NEXUS file of *Coelophysis bauri* specimens used for the sacral and pelvic character ontogenetic sequence analysis. See attached NEXUS file.

Data S10. NEXUS file of *Megapnosaurus rhodesiensis* specimens used for the sacral and pelvic character ontogenetic sequence analysis. See attached NEXUS file.

Data S11. NEXUS file of *Coelophysis bauri* specimens used for the suture fusion character ontogenetic sequence analysis. See attached NEXUS file.

Data S12. NEXUS file of *Coelophysis bauri* specimens used for the bone scar character ontogenetic sequence analysis. See attached NEXUS file.

Table S1. Measurements taken from *Coelophysis bauri* specimens.

Table S2. Measurements taken from *Megapnosaurus rhodesiensis* specimens.

Table S3. Linear regressions used to estimate femoral length for *Coelophysis bauri* and *Megapnosaurus rhodesiensis*.